THE PENNSYLVANIA STATE UNIVERSITY
SCHREYER HONORS COLLEGE

DEPARTMENT OF CHEMICAL ENGINEERING

FIRST PRINCIPLES AIRLIFT PHOTOBIOREACTOR FOR THE ENERGY BALANCE OF MICROALGAE FOR BIOFUELS APPLICATIONS

LUCAS ALEXANDER NUGENT
SPRING 2020

A thesis
submitted in partial fulfillment
of the requirements
for a baccalaureate degree
in Chemical Engineering
with honors in Chemical Engineering

Reviewed and approved* by the following:

Dr. Wayne Curtis
Professor of Chemical Engineering
Thesis Supervisor

Dr. Ali Borhan
Professor of Chemical Engineering
Honors Adviser

* Electronic approvals are on file.

ABSTRACT

For better feedstock selection of microalgae towards commercial biofuels and co-products, direct comparison of microalgae species via photosynthetic efficiency (PE) is needed to maximize solar-to-biomass energy conversion in an economically viable manner. PE is defined herein as the percentage of chemical energy converted into biomass from light energy absorbed in the photosynthetically active radiation (PAR) range. In this work, a novel photobioreactor (PBR), dubbed the 'Alginator', was designed and built to enable evaluation of any microalgae's PE under conditions that enable high-density, light-limited growth. A first principles approach was then taken to validate the Alginator's suitability for such an analysis using the common biofuels candidate, *Chlorella vulgaris.*

The Alginator was designed as a flat-panel airlift PBR. The flat-panel design was intended to support light limitation and provide straightforward calculation of PE by virtue of PAR flux measurements through a defined light path. The airlift design was intended to support high-density photoautotrophic growth through increased mass transfer and thorough mixing. These design elements were combined at bench-scale to promote ease of characterization and subsequent microalgal selection for commercial use.

For the Alginator's validation, the fluid dynamics of the system were first quantified using a dye tracer method for circulation time, fluid velocity, and flow turbulence. Next, the mass transfer of carbon dioxide into the reactor was characterized using a dynamic pH method to calculate the carbon dioxide mass transfer coefficient. Finally, *C. vulgaris* was grown in the Alginator towards providing both carbon mass and energy balances. Growth dynamics of *C. vulgaris* were characterized using optical density (OD) correlations. The combined carbon mass

transfer and biomass growth measurements enabled quantification of growth conditions throughout the batch trial. From there, dissolved oxygen (DO) conditions throughout growth were analyzed via the stoichiometrically determined photosynthetic reaction. For the energy balance, spectral analysis characterized absorbed photon energy while the biomass' total energy outputs were provided by the growth rate and bomb calorimetry measurements of energy density.

Finally, the resultant maximum calculated PE was 22% with an average of 8.8% throughout exponential growth illuminated with a PAR flux of $119 \pm 3 \frac{\mu E}{m^2 s}$. By comparison, literature values that calculate growth efficiency using PAR flux give a theoretical maximum PE of 27-29% in microalgae and experimental 9.0% for average PE throughout exponential *C. vulgaris* growth. Compiled results from literature show large discrepancies in reported PE for the same microalgae species with different PBR types, light conditions, and energy balance assumptions. In addition to Alginator characterizations, this thesis also highlights the need for relevant reactor conditions for scale-up and for consistency in assumptions when evaluating microalgae as a biofuels production platform.

TABLE OF CONTENTS

LIST OF FIGURES

ACKNOWLEDGEMENTS

I would first like to acknowledge Dr. Wayne Curtis for his continued support through this project. The Alginator idea was a brainchild of his, and he had a clear passion throughout this work to continuously strive for clear and meaningful results. Benji Geveke was an enormous help while he was working at Penn State, and much of this project would not have been possible without him. The original prototypes and CAD models were all with his significant input, and hours of glass-cutting attempts and silicone caulk failures taught me a lot about engineering, friendship, and teamwork. I would like to thank Ramya Mohandass for her support of this project during her time as a visiting scholar, including her sacrifices in taking some of the difficult nighttime sampling slots during algae growth. Thank you to Sarah Jean Johnson for her assistance in the pellet preparation and bomb calorimetry aspect of this work. Thank you to Andrew Sell who had a large part in the circulation time experiments, in particular bringing his Arduino and coding knowledge to the table when he was needed. Hinkal Patel and Mike Lind were critical in their assistance with this project and for helping to culture algae and contamination test when I was in need. Thank you also to Mick Price and Cindy Chen, and once again to Hinkal for their assistance and interest in continuing the Alginator work after my graduation. A big thank you to Erica Lennox for her support and knowledge, and for setting the example of what it looks like to work hard and stand up for yourself. Her big-picture contextualization of this work helped deliver more meaningful results and will likely lead to the motivation of subsequent Curtis Lab students in continuing this work for years to come. Thank you to all those who have supported me with “Algae Land” in Curtis Lab over the last five years, including Grant Gill, Ryan Jones, and Haonan Xu who helped train me in the summer of 2016

when I arrived in the lab. The picture below shows Ramya (left), Benji (left-center), me (right-center), and Grant (right) who helped push through the many challenges to get this work off the ground. Shout out to Philip O'Connor and Kyle McIlroy who kindly led me in the right direction for my Excel data smoothing techniques in the circulation time analysis after hours of frustration.

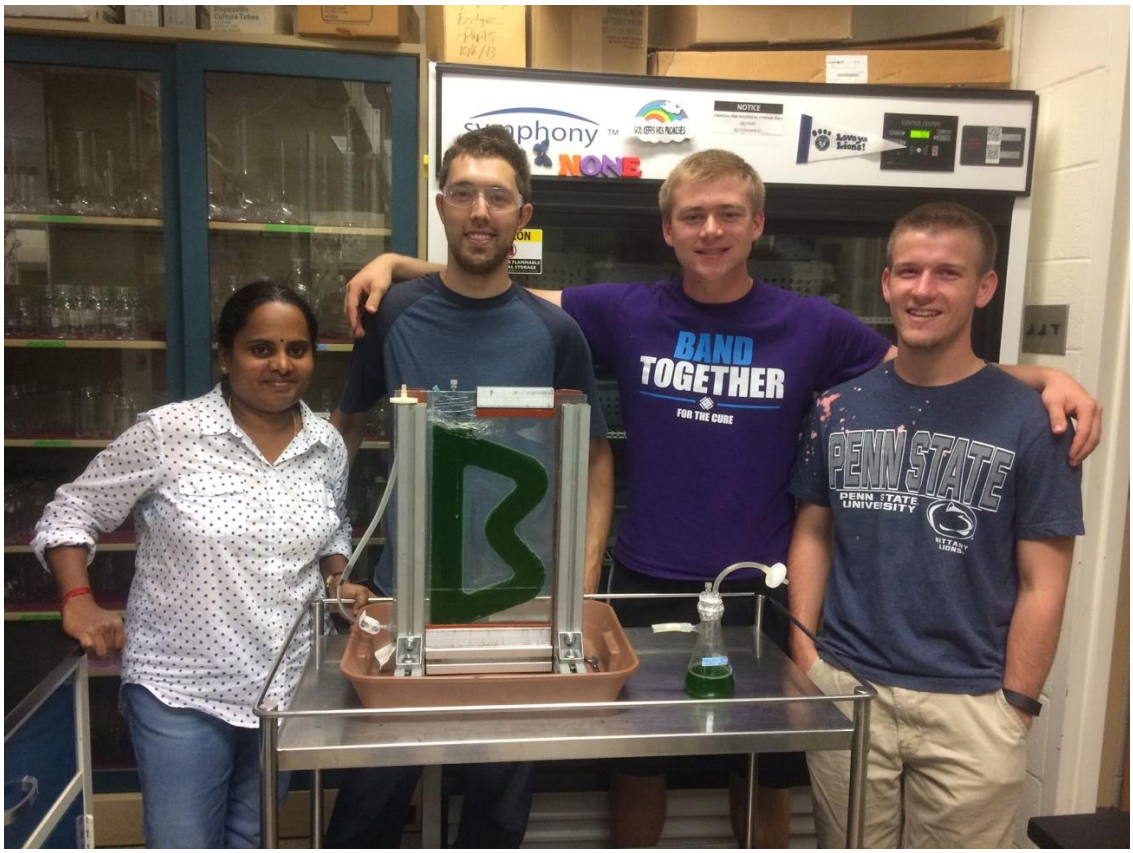

Finally, as I finish this thesis quarantined in my house during the COVID-19 pandemic, I would like to thank all my family and friends for their love and support throughout my time at PSU.

KEY TERMS AND ABBREVIATIONS

Photobioreactor (PBR) – A vessel used to grow a photosynthetic species, often microalgae, typically by providing light to a liquid culture through clear or opaque materials.

Alginator – The name given to the PBR that was designed, constructed, and characterized for the work of this thesis.

Microalgae – Unicellular photosynthetic micro-organisms, living in saline or freshwater environments, that convert sunlight, water and carbon dioxide to algal biomass.[1]

Chlorella vulgaris (C. vulgaris) – The species of microalgae cultured in this experiment; a common algae biofuels candidate.

Wayne's Freshwater Algae Media for Chlorella (WFAMC) – The *C. vulgaris* growth medium utilized in this thesis; developed by former Curtis Lab student Meg Scherholz.[2]

Photosynthetically Active Radiation (PAR) – The range of light generally accepted as usable in the photosynthetic process by chlorophyll; 400-700 nm.[3]

Biologically Accessible Photons (BAP) – The photons in the PAR range that are absorbed by the biological culture and can thus be used for photosynthesis. BAP calculation omits the light that transmits completely through the light path.

Photosynthetic Efficiency (PE) – Defined herein as the percentage of chemical energy converted into biomass from the light energy of BAP.

Carbon dioxide uptake rate (CUR) – The rate at which algae uptakes carbon dioxide during photosynthetic growth. Dependent on the biomass growth rate and composition.

Oxygen evolution rate (OER) – The rate at which the algae release oxygen during growth, stoichiometrically related to the CUR and dependent on growth conditions and media.

Volume/volume/minute (vvm) – A normalization term in bioreactor design that designates the volumetric flow of gas through a reactor. For example, a 2 mL/min gas flow into a 10 mL reactor volume would yield a vvm of 0.2.

Optical Density (OD) – A measure of light absorbance at a specified wavelength of a sample through a defined path length.

Overall volumetric mass transfer coefficient (k_La) – A key mass transfer parameter for the transfer of gas-phase carbon dioxide into the liquid media.

Chapter 1

Background and Introduction

Algae biofuels background and research needs

The growing threat of climate change has pushed international economic, social, and environmental goals to include biofuels in the forefront of long-term energy plans.[4] Substituting biofuels for fossil fuels is considered to be a key method of meeting the world's energy needs while reducing greenhouse gas emissions. It is estimated that up to 50% of the world's energy demands for heat, electricity, and transportation fuel could be met by biofuels by 2050.[5] The first generation biofuel utilized edible feedstocks such as wheat, soybeans, and potatoes. The inefficiencies of these crops, coupled with the ethical dilemma of redirecting food crops to biofuels, pushed the field towards more sustainable and higher-efficiency organisms such as microalgae.[4] A key aspect in development is improving the energy balance of algae biofuels to produce more usable chemical energy per unit energy investment. Alongside challenges in finding affordable carbon dioxide and water sources, efficient growth and large-scale processing remain some of the most pressing issues in the field.[6]

A technoeconomic analysis (TEA) estimates the environmental impact, economic feasibility, and mass and energy balances of the process from algae to biofuel.[6] TEAs for algae biofuels often include high levels of error, largely due to the need to extrapolate data from highly variable lab-scale research.[6] In particular, extrapolation of the energy balance around microalgae growth is littered with uncertainty due the wide variety of growth methods and energy balance assumptions often utilized.[7] A key component these assumptions often ignore is that once light-limitation is achieved by a high density algae culture, the intrinsic growth rates are no longer

relevant – and yield on the available photons will then dominate productivity. One goal of this thesis is to provide a framework for quickly and accurately comparing the energy balance of microalgae species at bench scale with well-defined and tested assumptions. To better bridge the gap between bench-scale and large-scale production, the energy balance should be measured in a way that applies directly to scale-up efforts. Bench-scale photobioreactors (PBR), for example, are often closed and irradiated by artificial lights, while outdoor systems are generally open to the atmosphere and solar-irradiated.[4] Various assumptions and growth conditions, defined in detail throughout this thesis, help to normalize the results to account for these differences.

Algae biofuel production can be broken down into steps that include feedstock selection, cultivation, and processing.[8] The efficiency and scalability of all three steps must be improved if algae biofuels are to become an economically viable replacement for fossil fuels. The first step is selection of the alternative biofuel feedstock. Feedstock alternatives provided by algae depend on the organism's biosynthetic capabilities, which can vary greatly for microalgae, cyanobacteria, or macroalgae such as kelp or seaweed. The work of this thesis is intended to allow for better feedstock selection of microalgae or cyanobacteria through cultivation under relevant conditions.

Cultivation of algae is most commonly done using photoautotrophic methods, where algae photosynthesize with inorganic carbon sources to produce new biomass. Photoautotrophic growth can take place in closed PBRs, of which an extraordinary variety exists, or via open systems such as circular or raceway ponds. This work characterizes photoautotrophic growth of microalgae using a closed, batch, bench-scale PBR designed to support scale-up operations. For any biomass needs, the selected cultivation method must leverage the advantages and optimal conditions of the feedstock and integrate efficiently with downstream processing.[8]

Processing the feedstock to fuel is the final step in an algae biofuel process. There are many approaches to processing depending on the target product. While transportation biofuel is often the end goal, some research has suggested that small-scale niche markets may be a good first step in the economic feasibility for biomass.[4] These niche products include valuable compounds such as pigments and nutraceuticals with which traditional fossil fuels cannot compete.[6] While these niche products are not a focus of this work, subsequent work in the Alginator could be a characterized analysis of these niche products. Processing begins with harvesting and dewatering the biomass, then extracting the lipids, carbohydrates, and proteins from the biomass. Extracted components can then be converted into the desired product using chemical, biochemical, and thermochemical methods.[8]

Despite widespread interest in algae biofuels, large disparities and uncertainties exist in microalgae TEAs. For example, preliminary studies consolidating available data reflected a 50-fold range in the total costs for producing a gallon of triglyceride oil from algae.[9] This extraordinary range comes largely from inconsistent growth conditions and energy balance assumptions. The uncertainty prevents would-be investors from taking the risk of putting significant money into scale-up. Sensitivity studies have concluded that the near-term viability of algae biofuels depends on the ability to accurately quantify and compare the total energy and mass balances such that the economic viability can be better understood and improved upon.[9]

In an effort to consolidate research, prioritize funding, and expedite the timeline of algae biofuels, the U.S. National Renewable Energy Laboratory (NREL) developed several key factors for the TEA of feedstocks, fuels and co-products.[9,10] The list of key factors includes:

1. Minimize **capital costs** per unit of biofuel
2. Minimize **operating costs** per unit of biofuel
3. Maximize **biofuel production yield**

4. Minimize net **greenhouse gas footprint** per unit biofuel produced
5. Maximize net **energy balance**
6. Minimize net **water usage**
7. Minimize **land footprint** per unit of biofuel produced
8. Minimize **time required** to reach desired production volume
9. Minimize **investment needed** to reach desired production volume

It is important to note the dependencies each factor has on the others. Take, for example, the hypothetical case where a microalgae species is developed with twice the energetic productivity as a current species. The assumed impacts to the key factors would include:

1. **Lower capital costs** per unit biofuel, as the bioreactor size could be reduced.
2. **Lower operating costs** per unit biofuel, with a smaller bioreactor for higher production.
3. **Increased biofuel production yield**, per both time and energy required.
4. **Lower greenhouse gas footprint** per unit biofuel, with reduced energy expenditure.
5. **Increased net energy balance**, with better output from the same input.
6. **Lower net water use**, with more efficiently utilized media per unit energy output.
7. **Lower land footprint** per unit biomass, with better yield per bioreactor size.
8. **Lower time required** to reach the desired production value.
9. **Lower investment needed** to reach desired production volume, as investment decreases with capital and operating costs.

This example showcases the potential impacts of a yield improvement across all key factors, and a similar analysis could be done for a marked improvement in any process step.

This thesis follows the research of Curtis Lab members over many years that have investigated high density, light-limited growth of microalgae for feedstock selection. As early as 2004, Dr. Curtis successfully filed for a U.S. patent for the design of a recirculating trickle-film reactor for the purpose of biomass growth.[11] Theses by Lisa Grady in 2010 and Amalie Tuerk in 2011 investigated the impacts on lipid yield of *C. vulgaris* in comparison to *Botryococcus branuii* race B using a continuous trickle-film PBR on a pilot scale.[12,13] The work by Grady and Tuerk was co-dependent on research led by Brandon Curtis in development of the trickle-film reactor in the investigation of *Rhodobacter*.[14] These Curtis Lab theses highlighted issues inherent

in selecting microalgae feedstock by intrinsic growth rate rather than energy conversion efficiency. A key takeaway from the prior research was that counterintuitively, despite an order-of-magnitude difference in the growth rate, *B. braunii* achieved a higher energy productivity than the faster-growing *C. vulgaris*.

Khatri et al. (2014) continued this work with *B. braunii* race B on the trickle-film PBR at ultra-high concentrations.[15] The work by Khatri investigated the oil productivity of *B. braunii* under light-limited conditions. The results of that work once again highlighted the importance of relevant cultivation conditions, resulting in oil productivity values an order of magnitude higher than previously accepted values for *B. braunii*. It was hypothesized that the dramatically better results were due to these light-limited, high density conditions in contrast to assumptions drawn from shaker flask experimentation under nutrient or carbon-limited growth.[15]

The Curtis Lab trickle-film work was submitted to Nature Biotechnology in a communication entitled “Algae Biofuels: Slow and Steady Can Win” with collaboration from the National Energy Technology (NETL) and the University of Kentucky, but has not yet been followed up for publication.[16] This communication showed the slower-growing *B. braunii* outperforming *C. vulgaris* in energy capture productivity in the high-density, light-limited trickle-film system. This challenged the status quo where the faster growing algae species is often presumed to be better, and energy capture productivity under relevant cultivation parameters is largely ignored. Despite these results, few in the biological world or in commercial start-ups have taken note and applied the learnings in a meaningful way.

One hypothesis on why the “slow and steady” perspective has not taken hold in the biological community is the barrier to entry on constructing and validating a complex, pilot-scale, trickle-film reactor. Construction, validation, and operation of this equipment requires an

in-depth engineering approach that is not within the scope of interest for most biological laboratories or start-ups. Thus, the Alginator idea came from this need to simplify a system to replicate relevant cultivation conditions for microalgae comparison in an easily reproducible, highly characterized bench-scale system.

Chapter 2

Alginator: Design Requirements and Construction

Alginator design requirements

The design of the Alginator was aimed at enabling microalgae selection by creating a characterized photobioreactor (PBR) environment to compare photosynthetic efficiency (PE) in light-limited, high-density conditions. A clear set of conditions and assumptions were developed for the Alginator to allow for a more meaningful technoeconomic assessment (TEA):[10]

- Alginator PBR requirements
    - Characterized light via measured photosynthetically active radiation (PAR)
    - Constant and defined light path
    - Sufficiently mixed culture with characterized hydrodynamics
    - Light-limited conditions as confirmed with carbon mass balance
    - Reasonable-cost and reproducible design
- Assumptions
    - Operating conditions
        - Photoautotrophic growth
        - CO_2 supplementation
        - Monoculture of known microalgae strain
        - Microalgae growth regulated on a day/night circadian cycle
    - Energy balance calculations
        - Energy input is the energy of biologically accessible photons (BAP)
            - Only absorbed photons in the photosynthetically active radiation range (PAR) of 400-700 nm considered.[3]
                - BAP is relevant to solar-illuminated scale-up because it normalizes for reactor geometry and light source.[17,18]
        - Energy output is the chemical energy of biomass.
        - Energy balance is reported as a simple ratio of energy output over input.

A flat-panel, external-loop airlift PBR was determined to be suitable to meet these needs.[19] The flat-panel design allows for a flux analysis with constant and defined light path, and an approximated 2D illuminated flat surface on each side. An airlift PBR has a circulating liquid

flow driven by gas through a porous sparger. The sparger serves the dual purposes of carbon dioxide supplementation (to support biomass growth and pH buffering) as well as driving flow. In an external-loop airlift system, gas rises up a vertical section called the riser. The lower density of the riser (with approximated 10% gas holdup) allows liquid in the downcomer section to flow downward, driving a constant flow. Along with the power of the rising bubbles, this density differential both creates flow and mixes the culture.[20] The final design of the Alginator is shown in **Figure 1**. The zig-zag design of downcomer section allows for better utilization of the available space, while the riser is vertical to allow bubbles to rise evenly.

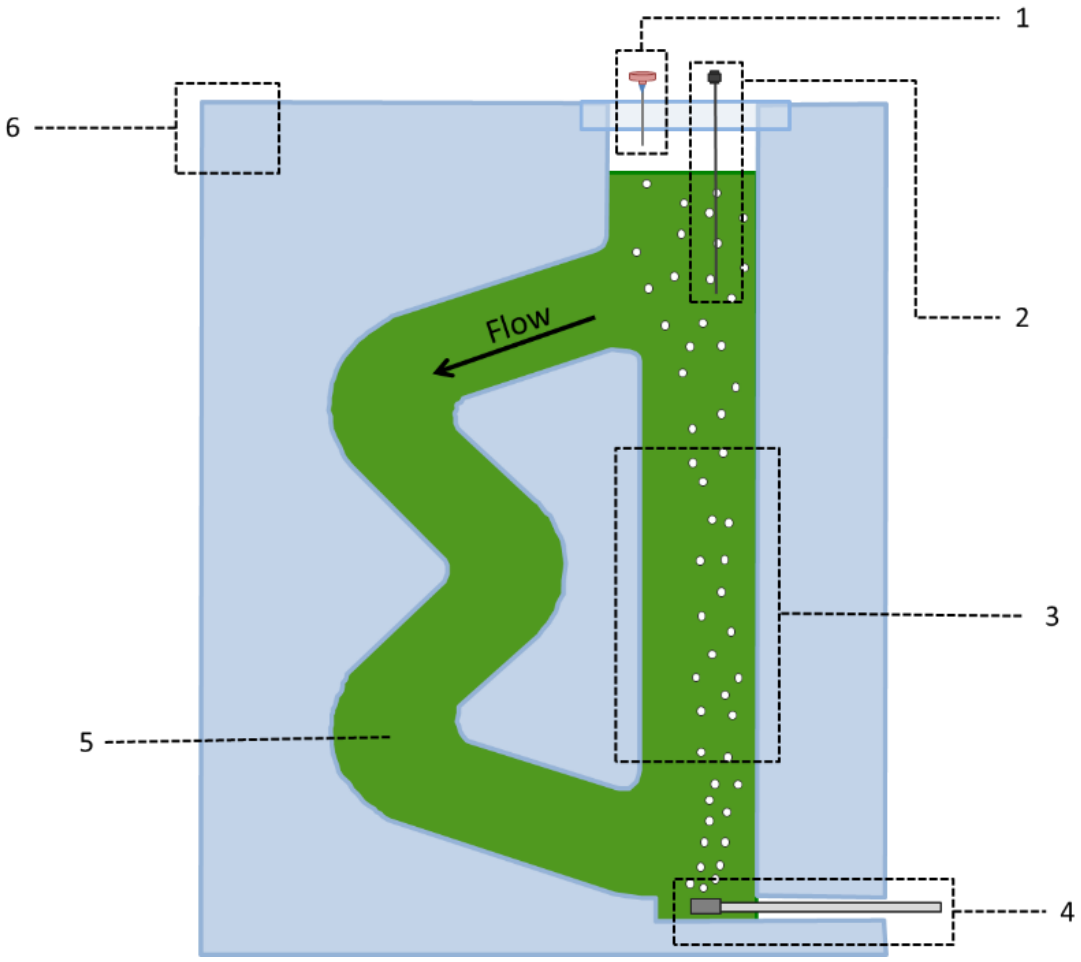

Figure 1: Design of the Alginator: 1) Filter attached to needle facilitates head-gas release into atmosphere 2) A tubular cannula is used as a sampling port 3) Riser column, 10% wider than downcomer for gas holdup 4) Gas sparger that drives flow and enhances mixing 5) Downcomer section 6) Defined light path consisting of an acrylic center surrounded by glass panes.

The microalgae strain *Chlorella vulgaris* was selected for the first principles characterization. *C. vulgaris* is a relatively fast-growing strain (doubling time 3-6 hours) without the added complexities of an extracellular lipid matrix that other strains of interest, such as *Botryococcus braunii*, develop during growth.[21] The next several chapters each address a component of this first principles approach, with characterizations of Alginator hydrodynamics, *C. vulgaris* growth, carbon and oxygen mass transfer, and energy balance.

Alginator materials and CAD model

With the exception of a $4 glass cutter used to manually cut the glass panes, all materials were found in the Lion Surplus Thrift Store dumpster or scavenged from historic Curtis Lab projects. The complete list of materials for construction is as follows:

- Two panes of 1/8 inch thick annealed glass, cut to 48x32 inches
    - Can be cut from larger panes using YouTube tutorials
        - SOP for glass cutting developed my Benji Geveke and myself can be found at this link: https://www.youtube.com/watch?v=1wMA66tNN-w
    - Important to use annealed rather than tempered glass for ease of cutting
- One pane of 3/8 inch thick acrylic, 48x32 inches or slightly larger
- Access to a laser cutter capable of cutting the acrylic pane from a CAD model
- Silicone caulk (100% waterproof, 100% silicone, all-purpose 10.1 oz) with caulking gun
- Gas sparger – Ace Glass 7 mm outer diameter by 210 mm length, porosity B (70-100 micron) filter stick
    - Item #: 4158389

SolidWorks 2015 was used to model the Alginator, with the final model shown in **Figure 2**. To aid in the accessibility of this work, the CAD model is open source and available on the Curtis Lab website for download: http://www.curtislab.org/research-projects/algae#TOC-Alginator-for-Bench-Scale-Microalgae-Characterization-Based-on-Photoefficiency-Metrics

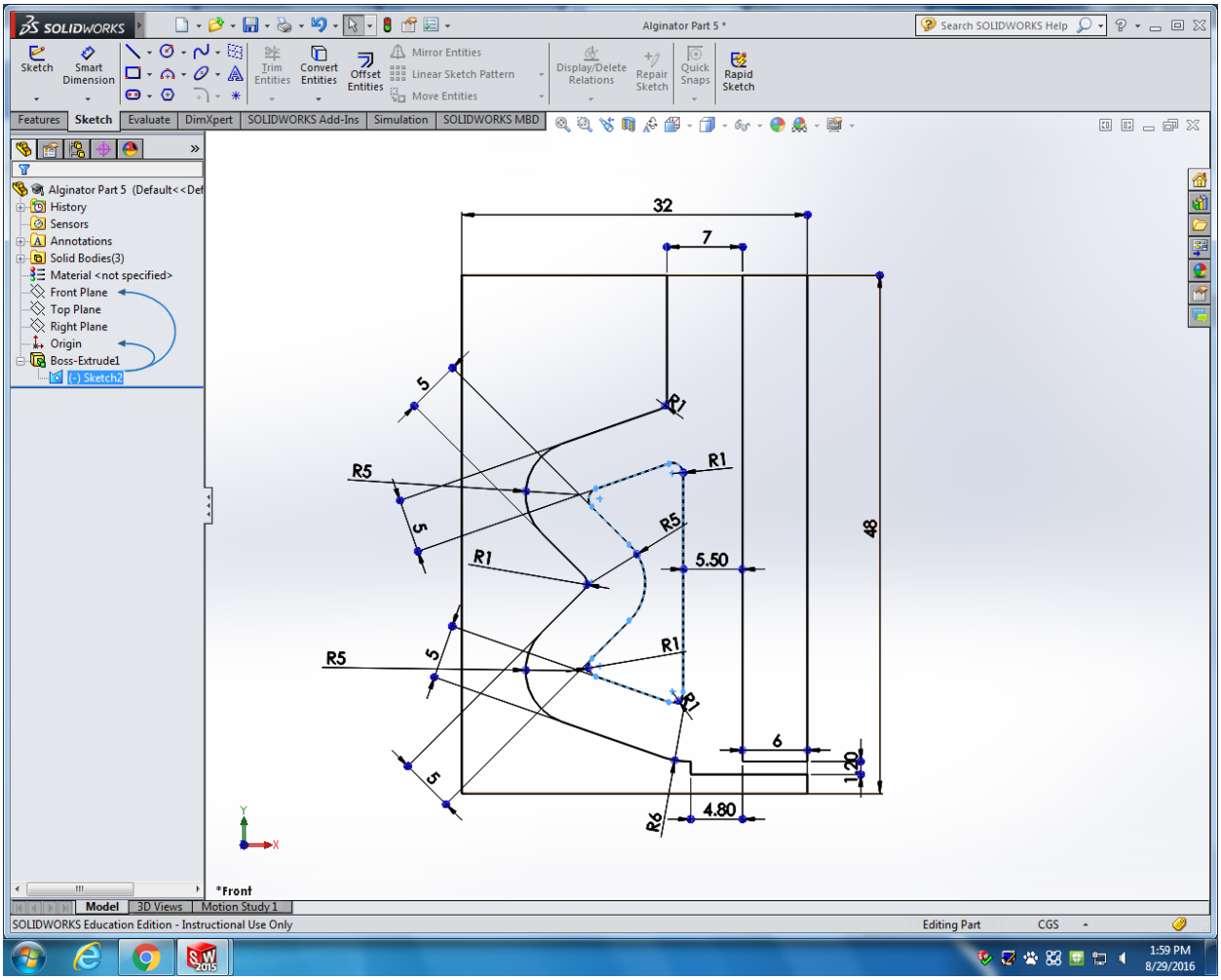

Figure 2: SolidWorks CAD model of the Alginator specifications for laser cutting, with dimensions in centimeters.

The open-source CAD model in **Figure 2** can be modified to meet volume, path length, or other needs for future projects. The flow path width is 5 cm in the downcomer and 5.5 cm (10% wider) in the riser section to account for the assumed 10% gas holdup in the riser. The head section of the Alginator is 7 cm wide; this widening helps mitigate the build-up of bubbles during operation. The extra head space above the path length also serves to prevent spillover of bubbles that occur at high biomass concentrations. Note that these biofilm bubbles are the reason for the hydrophobic plastic wrap cover rather than a sponge that was initially considered. With plastic wrap, the aerosolized culture with algae accumulates on the plastic and drips back in,

rather than accumulating as loss in the sponge. The total path length of the flow channel is 87.5 cm, with one third of the length accounting for the riser and two thirds the downcomer. The entrance in the bottom allows for securing the sparger underneath the riser section.

Alginator construction

The Alginator SolidWorks Part was exported as a DXF file for laser cutting at the Penn State Learning Factory. The final laser-cut acrylic pane is shown in **Figure 3**, where the acrylic comprising the Alginator is separated into three distinct pieces to create the desired flow path.

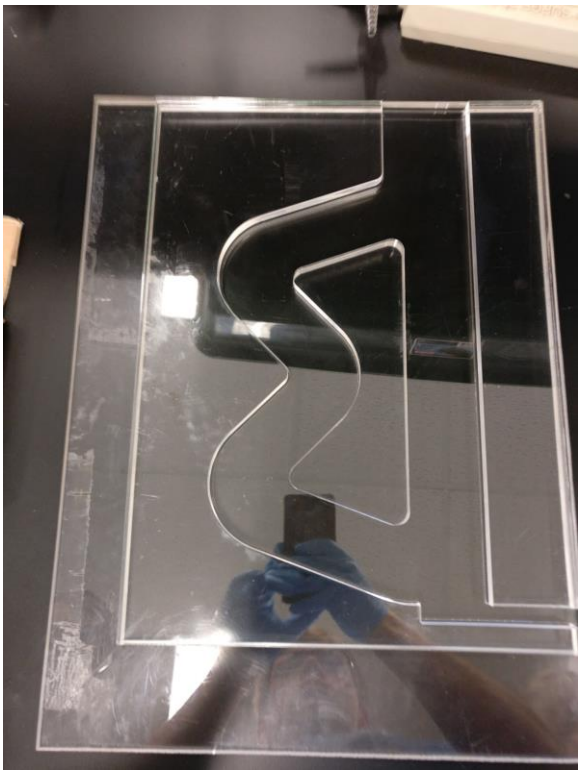

Figure 3: Laser-cut acrylic pane into three distinct pieces, making the Alginator flow path. Completed at Penn State Learning Factory (https://www.lf.psu.edu)

To remove any particles, the acrylic pieces were first cleaned with soap and water, then allowed to dry completely. The acrylic pieces were then laid down on a bench top and a ruler

was used to place the three pieces into the correct orientation based on **Figure 2**. A thin, continuous layer of silicone caulk was applied to the top perimeter of each acrylic piece using the caulking gun. (Note: It is highly recommended to practice using the caulking gun before actual application. Any gaps in the continuous line of silicone caulk can lead to leakage in the final bioreactor assembly. Removing dried silicone caulk due to erroneous application is difficult and time-consuming.) Once the silicone caulk was applied and while it was still wet, a glass pane was placed straight down on top of the acrylic, compressing the caulk between the acrylic and glass and spreading slightly into the flow path. A wooden board, larger than the Alginator dimensions, was placed on top for even compression, and textbooks were used to apply constant pressure for the 24-hour drying time. The construction after this stage can be seen in **Figure 4**.

Figure 4: Partially-constructed Alginator with one sheet of glass attached to acrylic, and displaying the silicone caulk with caulking gun and sparger used in the setup.

The Alginator was then flipped and the same method was used to secure the second pane of glass onto the other side of acrylic. Since it is no longer possible to gain access to the inside of the flow path after assembly of the second external glass panel, it is very important to apply the 'correct' amount of silicone – which is based on the experience of affixing the first glass panel to the internal flow path pieces. The sparger was also secured in place using silicone caulk during this step. This was done by filling the sparger entrance space with caulk and centering the sparger within the flow channel such that it was suspended via silicone between the glass and acrylic surfaces. Care was taken to not get any silicone caulk on the porous end on the sparger. The final measured thickness of the flow path was 1.0 cm, with the side profile shown in **Figure 5**. An effective volume of 430 mL was determined, representing a liquid height approximately one inch into the head section above the downcomer entrance. At 430 mL, the surface area of liquid exposed to light on from each side was calculated to be 0.0423 m^2.

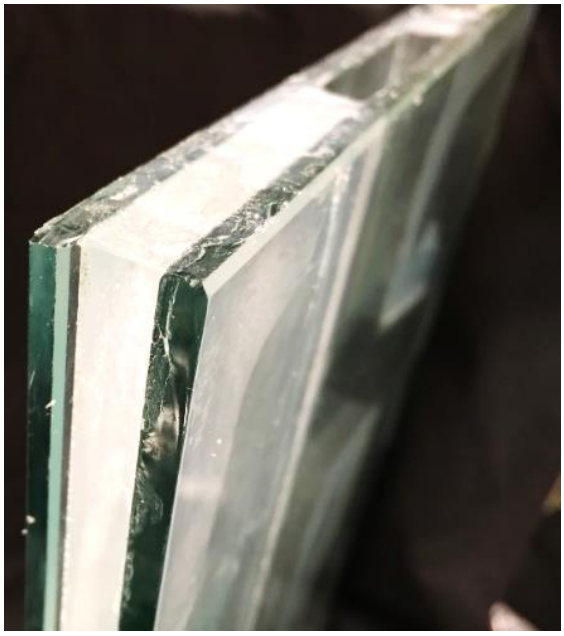

Figure 5: Side view of the Alginator, displaying the two panes of glass surrounding acrylic. The light path is 1.0 cm.

Chapter 3

Characterization of Alginator Hydrodynamics

Materials and methods

Understanding fluid flow dynamic aids in predicting and modeling the ways that microalgae behave in a photobioreactor (PBR). The method used to determine the circulation times and mixing properties of the Alginator was modeled from a method used by Musial et al. (2014) for a similar external-loop airlift PBR.[22] The setup of their reactor is shown in **Figure 6**.

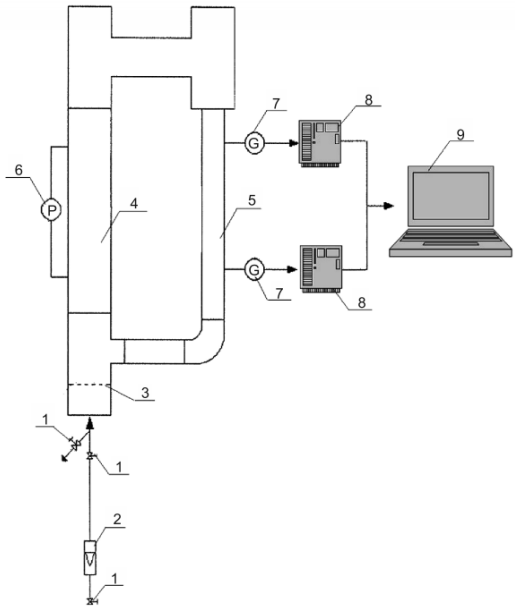

Figure 6: External-loop airlift bioreactor adapted from Musial et al. (2014) under international creative commons license.[22] The scheme of their external-loop airlift PBR is: 1 – valve, 2 – rotameter, 3 – gas sparger, 4 – riser, 5 – downcomer, 6 – inverted-tube manometer, 7 – electrode for measurement of conductivity, 8 – laboratory meter, 9 – computer.

To measure the circulation time, the researchers inserted a pulse of sodium chloride solution into the PBR while conductivity probes measured the change in conductivity over time during circulation. The period of oscillation between relative minima of conductivity represents one circulation period, t_c. **Figure 7** displays an example pulse time course from the work of

Musial et al. (2014) where G represents conductivity and t represents time. The solution disperses as the reactor circulates, with each subsequent peak decreasing in intensity until a steady state is reached. The time to reach the new steady state is the dispersion time. Results from **Figure 7** show a power law trendline over the range of gas flow rates.[22]

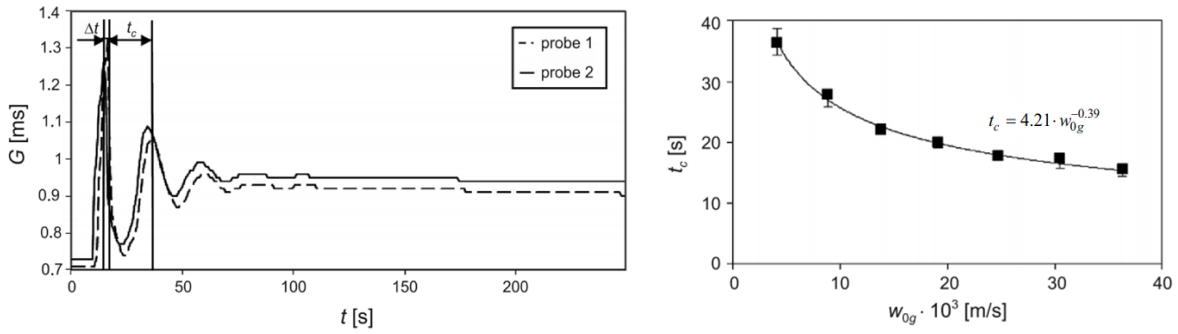

Figure 7: Results adapted from the work of Musial et al. (2014) under international creative commons license[22] Left: Pulse profile of a conductive solution in the external-loop airlift reactor setup depicted in **Figure 6**, measuring conductivity (G) versus time (t). Right: Compiled results and power law trendline depicting liquid circulation time (t_c) versus superficial gas velocity (w_{0g}).

An adaptation of this method was utilized to characterize hydrodynamics in the Alginator. Rather than a conductive solution pulse, an absorbent dye was pulsed into Alginator as measured with photodiode and LED. The materials for this experiment are as follows:

- Alginator
- Calibrated rotameter to manually measure and adjust gas flow rate (Brooks 2-15D tantalum float – SN: 8802HC090513/2)
- Werther air compressor
- Silicone tubing
- Blue Dye FCF #1 (from grocery store, with peak absorption at 628 nm)[23]
- 627 nm Red LED (5 mm, Super Bright LEDs Part: RL5-R12008)
- Syringe with male luer connection
- Cannula (Cadence Science 316 SS 18 gauge, 6” canula with Micro-Mate® Hub, VWR Cat. No. 20069-038)
- PLX-DAQ data logging software
- Arduino Setup shown in **Figure 8** (constructed and coded by Curtis Lab undergraduate Andrew Sell)
    - Arduino Uno

- Photodiode (Texas Instruments OPT101 Monolithic Photodiode and Single-Supply Transimpedance Amplifier) with pin configuration as shown in **Figure 8**
- Small breadboard
- Male to male wires
- 100 ohm resistor
- 1 Mohm resistor
- 100 μf capacitor
- 0.22 μf capacitor

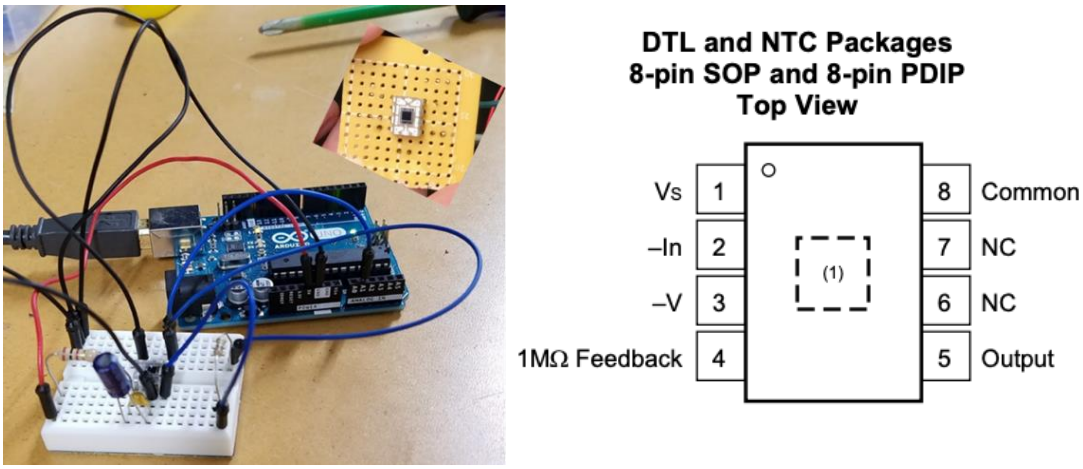

Figure 8: Left: The Arduino Uno mechanism and Opt101 photodiode (top right) to measure relative photon flux. Right: Pin configuration of the Opt101 photodiode from Texas Instruments.[24]

Step-by-step directions for the photodiode setup are as follows:

1. Connect ground (3 and 8) to ground
2. Connect pin 1 through a 100-ohm resistor to +5V
    a. This reduces the noise in the power supply
3. Connect the 100 μf capacitor from pin 1 to pin 3
    a. Negative leg goes towards ground (pin 3) and positive leg towards 5V (pin 1)
4. Connect the 0.22 μf capacitor from pin 1 to pin 3
5. Connect pin 5 to pin 4 with 1 Mohm resistor
    a. The sensitivity can be altered by changing the resistor value here
6. Connect pin 5 to Analog A1 on Arduino
7. Run the following code on PLX-DAQ software, with output into Microsoft Excel:

```
void setup(void) {
 Serial.begin(9600);
 Serial.println("CLEARDATA");
 Serial.println("LABEL,Time,Timer,Voltage,");
 Serial.println("RESETTIMER");
```

```
}
void loop(void) {
 Serial.print("DATA,TIME,TIMER,");
 int sensorValue = analogRead(A0);
 float voltage= sensorValue*(5.0/1023.0);
 Serial.println(voltage);
          delay(100);
}
```

The complete experimental configuration is shown in **Figure 9**. The LED was secured opposite the photodiode along the downcomer. Using the cannula attached to the syringe, a pulse of blue dye was introduced into the Alginator in the location depicted in **Figure 9**. With the Arduino setup described above, relative time course light readings as voltage were sent to PLX-DAQ and logged in Excel. The pulse was repeated in triplicate through a range of gas flow rates from 0.077 to 0.477 vvm. **Figure 9** also includes the dispersed steady state after the dye pulse.

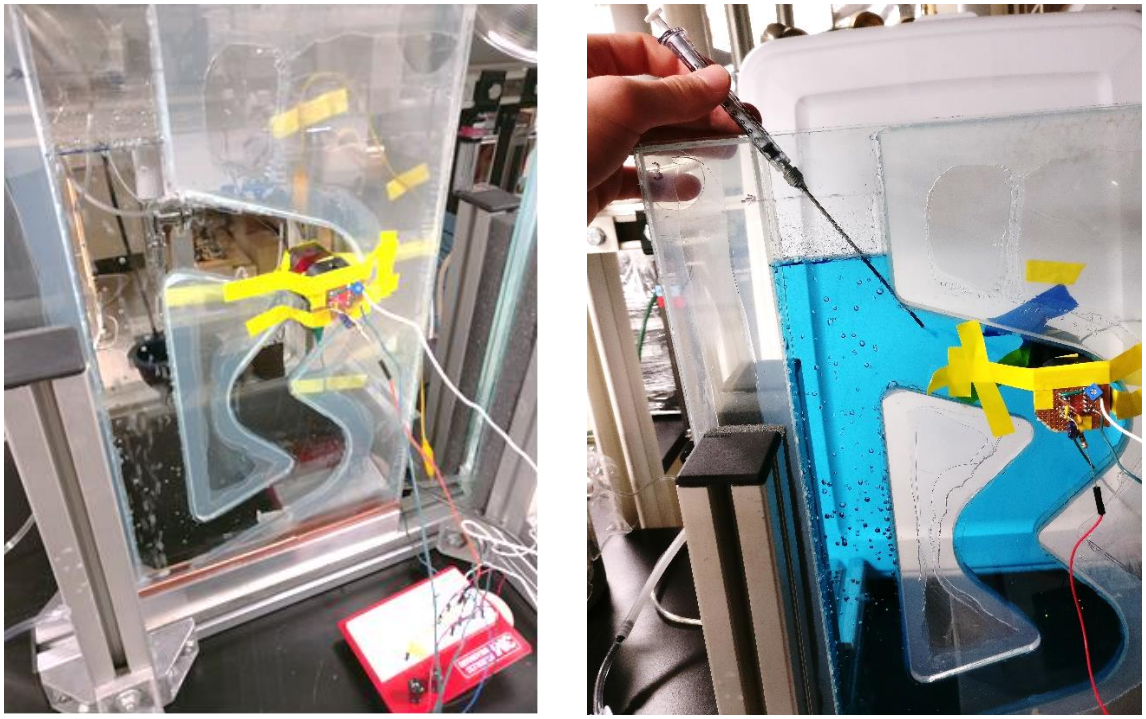

Figure 9: Left: Photodiode and LED setup on the Alginator for circulation time measurements. Right: Syringe with attached cannula at the dye insertion point after steady state was reached.

Circulation time and liquid velocity results and discussion

In agreement with the results from Musial et al. (2014), each dye pulse produced a decreasing amplitude wave where the period of the wave represents the circulation time and the time from pulse to steady state represents dispersion time. Because the dye absorbs light before it reaches the photodiode, a higher concentration of dye between the LED and photodiode represents a lower voltage reading. **Figure 10** shows the results from one dye pulse at a vvm of 0.278. To extract circulation time data from the raw time course voltage readings, a moving average trendline was calculated for each data set. A moving average trendline is a method of obtaining a smooth continuous trend from periodically sampled data. This was done using the Moving Average trendline feature in Excel and selecting a period between 10 and 15, depending on the relative noisiness of the trial. The graph in **Figure 10** includes a 0.45 second leftward correction of the trend line to account for drift that is common with moving average trendlines. Local extrema data were then obtained based on the trendline, where the difference in x values (time) between minima or maxima indicate circulation time.

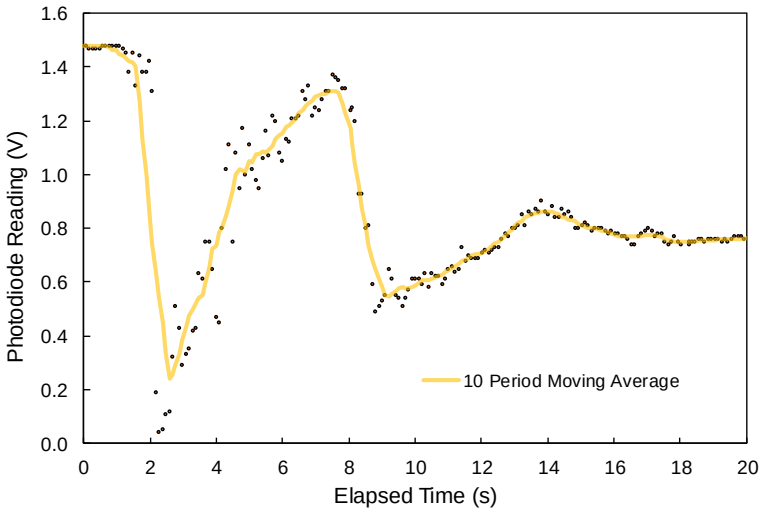

Figure 10: Example time course at a vvm of 0.278 with a blue dye pulse in the Alginator, as measured by the setup depicted in **Figure 9**. A circulation time of 6.5 seconds was calculated for this example.

The circulation time results for each vvm were averaged, with mean values and standard error bars depicted in **Figure 11**. In alignment with the results from Musial et al. (2014), circulation time was well-modeled using a power law dependence of the circulation time on gas flow rate, yielding an R^2 of 0.991.

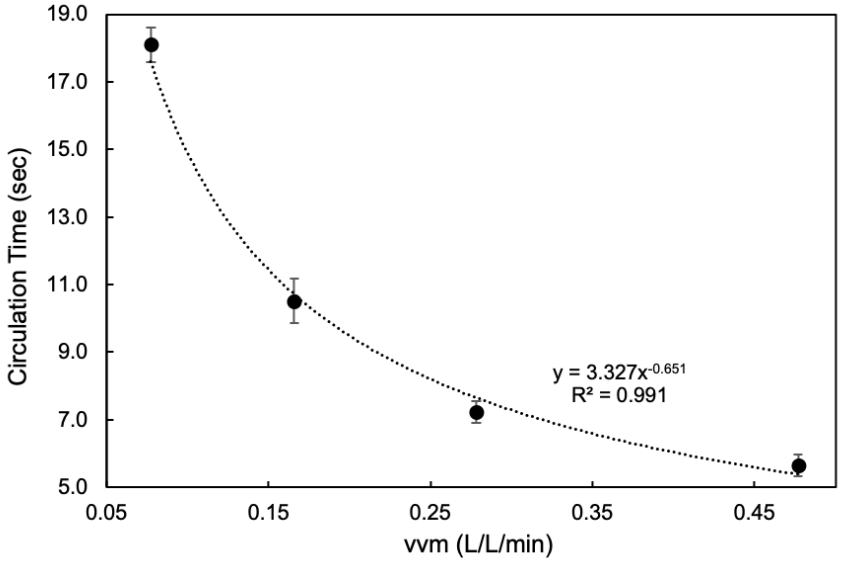

Figure 11: Circulation time in the Algaintor as a function of vvm. The power law trendline with R^2 of 0.991 indicates that the Alginator behaved similarly to the airlift reactor tested by Musial et al. (2014).[22]

Fluid velocity was calculated by dividing the total path length of 87.5 cm by the circulation time at each vvm. The results for fluid velocity versus vvm in the Alginator are shown in **Figure 12**. The liquid velocity profile fits a logarithmic dependence of the average circulation velocity with increasing gas flow rates, with an R^2 of 0.990.

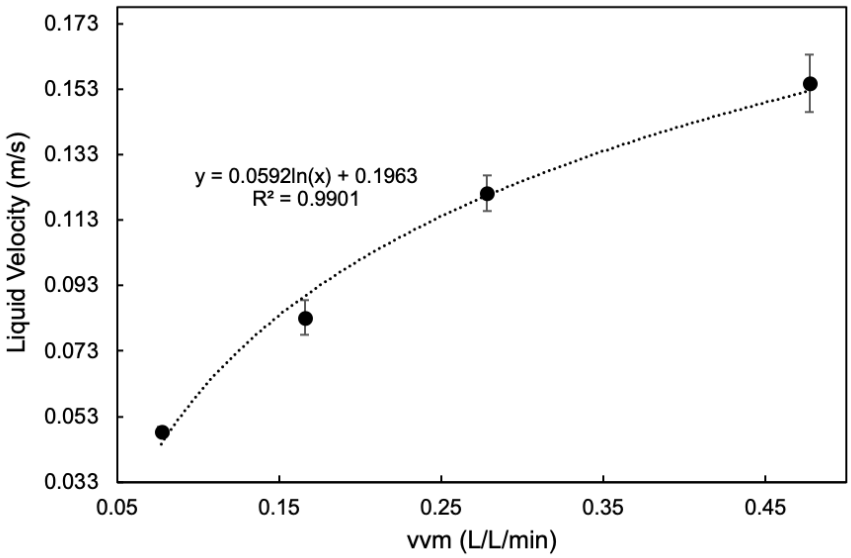

Figure 12: Fluid velocity in the Alginator as a function of vvm, with error bars representing standard error.

Reynolds number calculations

Visual observations confirmed good dispersion through the Alginator at all gas flow rates tested. A Reynolds number was calculated for each flow rate to more quantitatively characterize the flow condition. The Reynolds number is a dimensionless parameter that gives insight to the qualities of flow, in particular the level of turbulence. It compares the ratio of inertial to viscous forces within a fluid, and it is generally considered that a Reynolds number below 2100 (in pipe flow) represents laminar flow and above represents turbulent flow.[25]

For perspective on the Reynolds number analysis, it is important to note that an airlift PBR has some distinctly different characteristics to standard pipe flow. First, the flow path is 'channel flow' with an intentionally high aspect ratio (very thin in the light path dimension) as required for the intended purposed of calculating light use efficiency. In addition, this is not single-phase fluid flow. The Brownian motion of the rising bubbles adds mixing forces to the

flow that would not be observed in a simple one-phase system.[20] This two-phase flow allows airlift PBRs to be operated at lower Reynolds numbers than most other reactor types. An analysis by Croze et al. (2013) found that airlift PBRs could often be efficiently operated at Reynolds numbers as low as 100, while efficient raceway ponds and tubular reactors exhibited Reynolds numbers often on the order of 30,000.[26] Computer simulations for the fluid dynamics of a flat-panel external-loop airlift PBR were developed by Hassanzadeganroudsari et al. (2018).[20] In that study, the researchers suggest that mixing within the reactor is significantly improved by the movement of turbulently rising bubbles through the riser section. As additional mixing forces in the Alginator flow path, Dean vortices are also expected to occur in the downcomer section, as a function of centrifugal forces in the zig-zagging flow path.[27]

The Reynolds number is calculated using,

$$Re = \frac{\rho v D_e}{\mu} \qquad \textbf{Equation 1}$$

where Re is the Reynolds number, v is liquid velocity, ρ is the fluid density, D_e is characteristic 'hydrodynamic' diameter, and μ is dynamic viscosity. In the case of rectangular pipe flow such as in the Alginator, D_e is the mean hydraulic diameter,

$$D_e = \frac{4 * cross\ section\ of\ fluid\ in\ the\ channel}{perimeter\ in\ contact\ with\ the\ fluid} = \frac{4 * y * z}{2 * y + 2 * z} \qquad \textbf{Equation 2}$$

where y is the width of the flow channel and z is the thickness. The Reynolds number was calculated using the downcomer section of the Alginator, where it is more representative of classic pipe flow than the bubble-filled riser section. The Alginator downcomer width is 5.0 cm and thickness 1.0 cm.

Calculation with **Equation 2** yielded a hydraulic mean diameter of 1.7 cm. The density and kinematic viscosity of water at room temperature were taken to be 998.2 kg/m^3 and 1.0

centipoise respectively.[28,29] Due to the relatively small fraction of biomass in the liquid even at high concentrations, the flow during microalgae growth was assumed to be well-modeled using properties of water as a basis. Utilizing **Equation 1**, the calculated Reynolds number at each vvm are graphed in **Figure 13**. Since all parameters are assumed constant in **Equation 1** with the exception of liquid velocity, the Reynold's number follows a logarithmic relationship consistent with **Figure 12**.

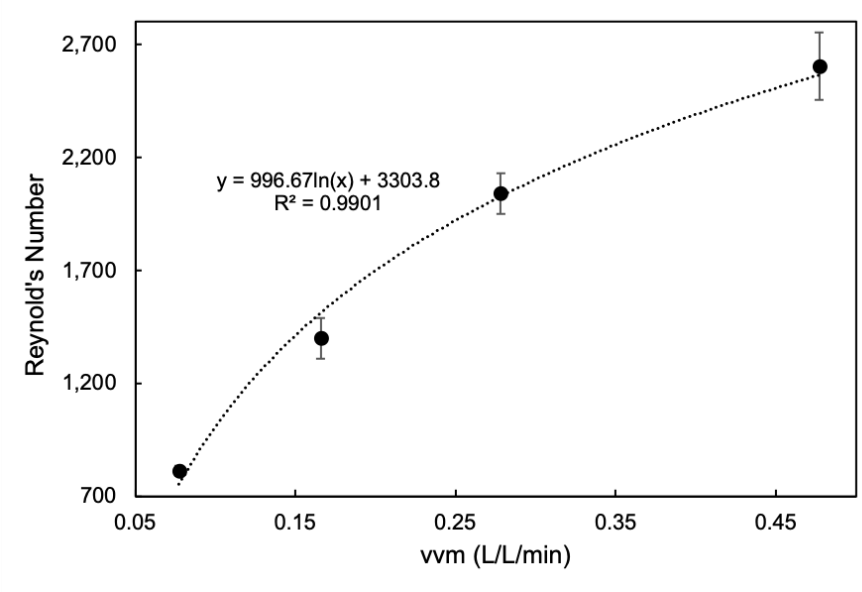

Figure 13: Dependency on vvm in the Alginator of the Reynold's number predicting fluid flow characteristics. The error bars represent the standard error of the mean.

Calculated Reynolds numbers ranged from 800 to 2600 in the vvm range tested of 0.077 to 0.477. A moderate vvm of 0.2 was selected for Alginator operation. At 0.2 vvm, the corresponding values for Reynolds number, liquid velocity, and circulation time would respectively be 1700, 0.1 m/s, and 9.5s. With one-third of the flow path as the riser and two-thirds as the downcomer, this translates to 3.2 seconds in the riser and 6.3 seconds in the downcomer section. One possible step for future analyses would be to use the circulation time correlations to further quantify mass transfer, because there are zones of high mass transfer in the

riser as compared to the nearly bubble-free downcomer. The analysis of mean residence times in the riser and downcomer sections would ensure no significant carbon dioxide depletion or oxygen accumulation take place in the flow path. Note that the accumulation of oxygen, and its suppression of photosynthetic efficiency due to increased photorespiration, has been acknowledged as a limiting factor in large scale algae bioreactor productivity.[30] Huang et al. (2017), for example, reported that high dissolved oxygen levels (greater than 200% of the air saturation value) can severely limit cell growth, particularly in closed reactors such as PBRs.[30]

Chapter 4

Growth of *Chlorella vulgaris* in the Alginator

C. vulgaris growth methods and materials

Media preparation

The media utilized in this experiment was Wayne's Freshwater Algae Media for Chlorella (WFAMC), developed by Curtis Lab student Meg Scherholz using biomass composition.[2] **Appendix A** shows the detailed chemical composition of WFAMC.

Gas delivery system

A gas delivery system was set up to provide carbon dioxide-enriched air to the Alginator and maintenance cultures of microalgae. A Werther air compressor was used to send air through an oil filter and into a rotameter (Brooks 2-15D Tantalum Float, SN: 8802HC090513/2). A carbon dioxide tank sent pressurized carbon dioxide into a separate rotameter (Brooks 2-15-AAA Glass Float). The flows of air and carbon dioxide were combined to create a 2.5% carbon dioxide gas mixture in air. After mixing, the gas stream was passed through a humidification train, shown in **Figure 14**. The purpose of the humidification train was to saturate the gas flow with water vapor such that the growth media was not stripped from the culture during operation. The humidification train, as was developed for previous Curtis Lab work, consisted of four connected flasks with deionized water in series and a sparger in each flask.

Figure 14: Humidification train to avoid liquid losses during growth.

From the humidification train, mixed gas was sent to a final rotameter (Brooks 2-15-A SN: 9203HC090812/3), at a vvm of 0.2 then through a Pall bacterial air filter (VWR Part #28145-553) prior to entering the Alginator. Excess gas was vented to allow for balancing the overall gas delivery system.

Culture maintenance of Chlorella vulgaris

Maintenance of *C. vulgaris* cultures was conducted on a gyratory shaker at 100 rpm. The cultures were grown in 250 mL of WFAMC media in 500 mL Erlenmeyer flasks. 2.5% carbon dioxide in air was passed through the cultures at a vvm of 0.2 using the daisy chain method shown in **Figure 15**.[15] Notably, since mass transfer in a shake flask is provided by agitation (not gas flow) the gas flow through these flasks does not have to be highly accurate – a simple confirmation of no leakage with flow out of the last flask on the daisy chain is adequate. Aseptic

technique was used to maintain the cultures, and the gas flow was sterilized using Pall bacterial air filters (VWR part # 28145-553) prior to entering the cultures. The exit tube was stuffed loosely with a small amount of cotton before flask sterilization to prevent contamination. The temperature for all samples was the laboratory room temperature of approximately 22˚C.

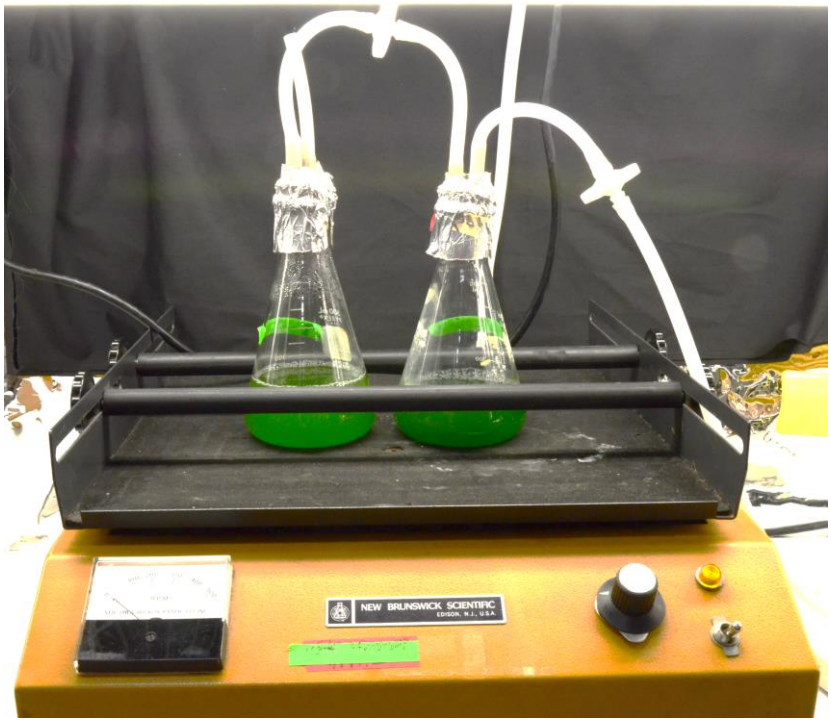

Figure 15: Culture maintenance setup and gyratory shaker for *C. vulgaris*, showing the daisy chain method.

This maintenance culture setup was the same as used for the control study, except with a 250 mL flask and 100 mL of liquid culture. Fluorescent lighting was measured on the surface of the gyratory shaker to be 60 $\frac{uE}{m^2 s}$ of photosynthetically active radiation (PAR) flux, where one Einstein (E) is equal to one mole on photons. Photographs of the light sensor logger (LI-COR LI-1500) and LI-COR quantum sensor for PAR flux measurements are shown in **Figure 16**.

Figure 16: LI-1500 Light Sensor Logger and LI-COR quantum sensor used to measure PAR flux

The microalgae were grown using a 16/8 diurnal light cycle, with carbon dioxide flow shut off during the night cycle to prevent toxic acidification. The time period of growth for this system is measured in photohours, considering only time during the day cycle when photosynthesis can occur. The importance of a day/night cycle was analyzed by De Winter et al. (2017) in which it was suggested that the day/night cycle is responsible for 'gating' cell division, respectively into growth during the light period and division during the dark period.[31] Using the species *Neochloris oleoabundans*, their work predicted that a day/night cycle provides a fitness benefit to microalgae by suspending cell division until night, where incident light energy that could be used for growth is not wasted during cell division. Their hypothesis was supported by measuring a 15% increase in energy efficiency (in units g biomass/mole photons) for the culture maintained on a 16/8 cycle rather than continuous.[31] The day/night approach also increases the relevance for scale-up, because economic scale-up relies on the natural sun cycle for light.

The housing constructed for the Alginator is shown in **Figure 17**. For lighting, a rack of four linear fluorescent lights (Philips Plus 800 Series Long Life T8 Fluorescent Lamp Type 32W F32T8/TL835/PLUS/ALTO, 3500K) was set up adjacent to the Alginator on both sides of the

flow path, totaling 8 lights. The Alginator was centered between these light racks with 18 cm separating each side of the Alginator from the bulbs. **Figure 17** shows a pane of glass representing how the Alginator fits into the housing during growth. To prevent photobleaching, only one of the two light racks was used for the first 16.5 photohours of growth. After this point, both light racks were utilized. To minimize photo-shock, the turn-on time for lighting in the racks was staggered by fifteen minutes.

Figure 17: A total of eight fluorescent bulbs (T8, 3500K) were used to provide light to the Alginator. A glass pane was used to simulate the Alginator flow channel for PAR flux analysis.

PAR flux into the Alginator was measured indirectly within the housing developed for Alginator work. The quantum sensor (shown in **Figure 16**) is larger than the thickness of the Alginator flow path, so PAR flux could not be measured directly inside the Alginator. Rather, a simple proxy was developed to measure PAR flux as would be received through the glass panes on either side of the Alginator flow path. The flow path was sketched onto a glass pane (in

Figure 17) and nine equally spaced points, shown in **Figure 18**, were measured for PAR flux through the glass from both light racks. No significant difference was found between the incident PAR light from each rack of lighting, and the average PAR flux measured was $119 \pm 3 \frac{\mu E}{m^2 s}$.

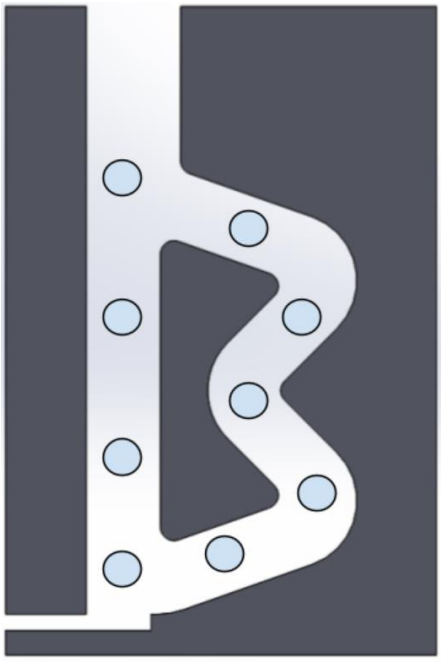

Figure 18: Locations at which the photon flux was measured. The average PAR photon flux onto the Alginator surface was measured as $119 \pm 3 \frac{\mu E}{m^2 * s}$.

Inoculation method for the Alginator and control

Inoculation of the Alginator was completed in a sterile fume hood, shown in **Figure 19**. Note that while a sponge in shown in **Figure 19**, the sponge was later replaced with plastic wrap taped to the top. This change was to prevent fluid from the popping sparged bubbles from being lost to absorption in the sponge. To sterilize the Alginator prior to the experimental growth, it was filled with a 10% bleach solution that was then passed through the sparger and into a waste bucket. A triplicate deionized and sterilized water rinse was used to clear the bleach.

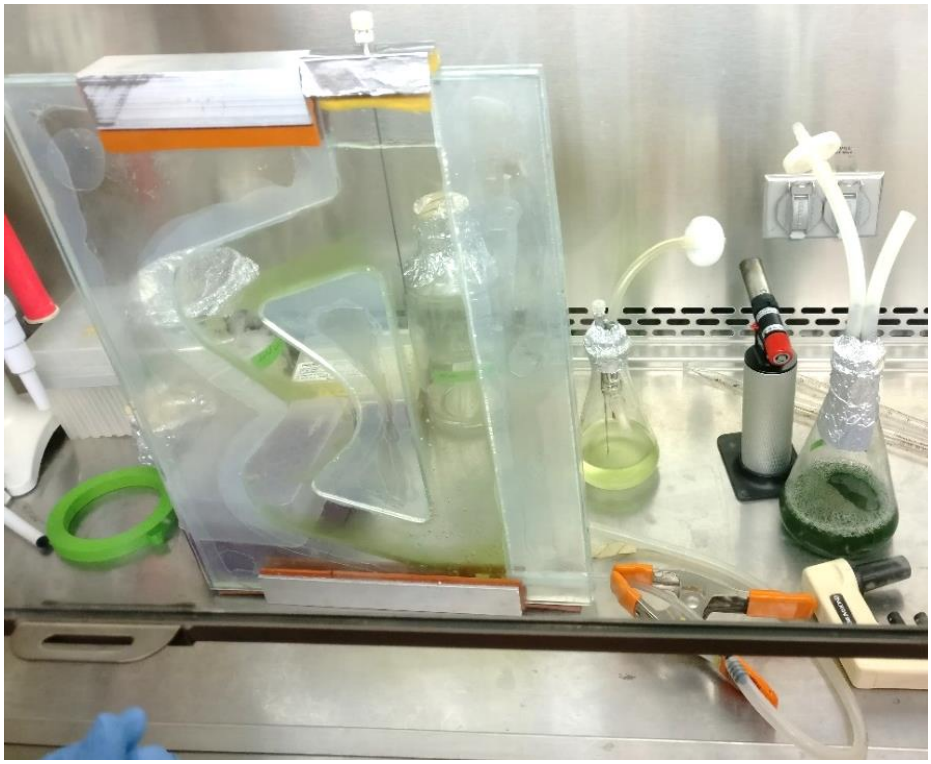

Figure 19: Inoculation of the Alginator in the fume hood, including the dense green parent culture and control flask.

OD is the measure of absorbance at a set wavelength through a defined path length. As a quick measure proportional to concentration, OD is often used to quantify microalgae and bacterial growth. The inoculated OD of the Alginator (at 430 mL) and control flask (100 mL) were both measured to be 0.1 at 550 nm.

Myers et al. (2013) investigated the OD method for quantifying growth.[32] Their work put forth the argument that each species has a robust OD measurement wavelength that does not significantly vary with changes to the biomass composition from growth in different conditions. In particular, changes to media composition or nutrient starvation can alter chlorophyll concentration and lead to erroneous mass correlations with OD. At wavelengths where sample light scattering is the main driver of optical density rather than chlorophyll absorption, the OD

measurements are more robust to biomass composition changes. For *C. vulgaris*, that robust wavelength was determined to be 550 nm.[32]

In this thesis, the OD was measured at high-sensitivity wavelength of 680 nm and the robust wavelength of 550 nm. Each sample was pulled directly from the cannula in the Alginator using a male luer syringe and measured non-aseptically in the Beckman DU520 spectrophotometer pictured in **Figure 20**. All samples were diluted with tap water to a 550 nm OD of 0.5 or below to enhance the linear correlation of the measurements within the measurement capabilities of the spectrophotometer.[32] To correct for the effects of liquid evaporation, sterile deionized water was added prior to each sample through the cannula to reach the initial liquid height point. Note this correction was done with air flow running, assuming a constant gas holdup throughout growth with the constant gas flow rate.

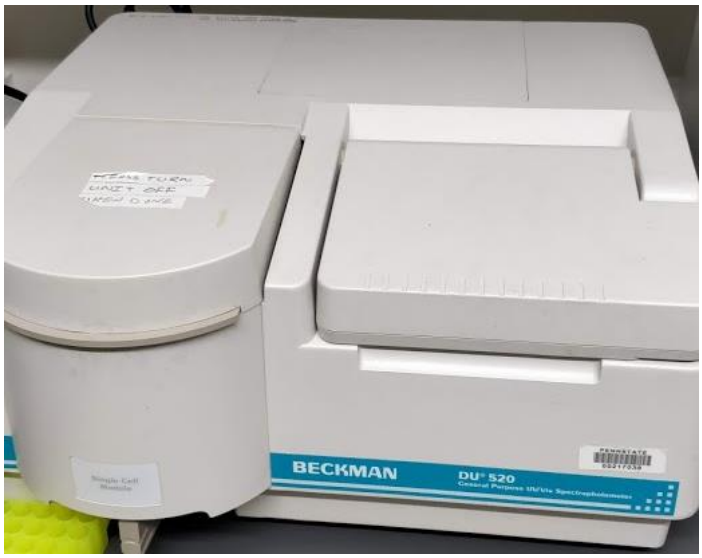

Figure 20: Beckman DU520 spectrophotometer used to measure the optical density of *C. vulgaris* throughout growth in the Alginator at both 550 nm and 680 nm.

Myers et al. (2013) also correlated the biomass of *C. vulgaris* suspended in liquid media to the 550 nm OD. Their correlation of 0.430 $\frac{\text{g biomass } C.\ vulgaris}{OD_{550} * L}$ was assumed to be accurate for

Alginator measurements.[32] Myers et al. (2013) concluded that these correlations must be made for each strain and with each spectrophotometer used. The correlation was considered accurate for the Alginator work only because the work by Myers et al. (2013) was completed on the same spectrophotometer. Note, however, that other studies of this relationship have yielded similar values for *C. vulgaris*, with Fu et al. (2012) for example reporting $0.42 \frac{\text{g biomass } C.\ vulgaris}{OD_{600} * L}$.[33]

C. vulgaris growth curve results and discussion

Growth of *C. vulgaris* in the Alginator is depicted in **Figure 21**, as characterized by the optical density (OD) at 550 nm and 680 nm for each sample point. **Figure 21** also shows the visual representation of the Alginator at inoculation and pre-harvest.

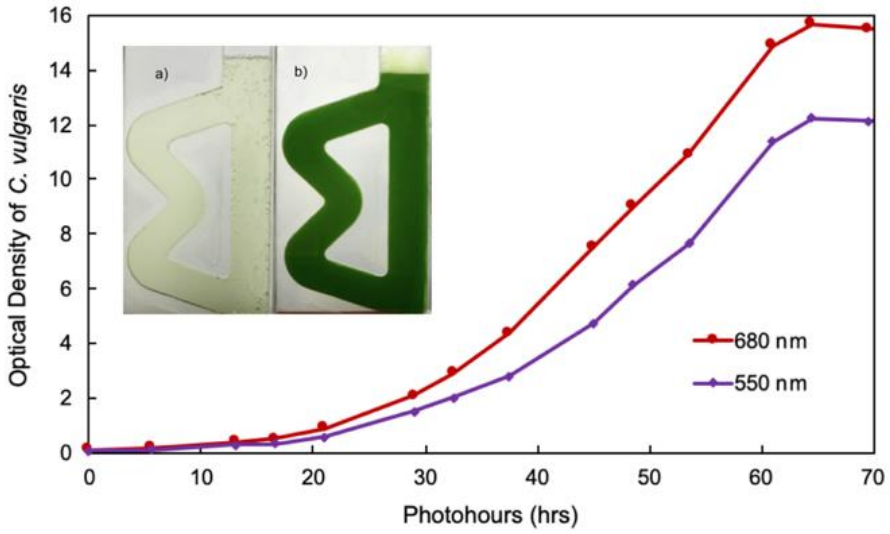

Figure 21: Growth of *C. vulgaris* in the Alginator at the robust wavelength of 550 nm and the high absorbance wavelength of 680 nm. Inset is the visual *C. vulgaris* growth at a) inoculation b) prior to culture harvest.

Oukarroum et al. (2016) investigated the growth of *C. vulgaris* in an aerated reactor at room temperature and found growth to be characterized by an exponential phase followed by a stationary phase.[34] Growth was exponential in the Alginator until approximately 61 photohours

at which point the culture transitioned into a stationary growth phase. This is the point at which nutrient-limitation was assumed to begin. The OD at 550 nm and 680 nm followed the same growth trend, with the 680 nm OD consistently measuring higher than the 550 nm. This difference is explained by the absorption of light by chlorophyll at 680 nm, with light scattering primarily dominating at the robust OD 550 nm.

Figure 22 shows the comparison of *C. vulgaris* growth between the Alginator and maintenance culture used as a control. At 61 photohours, the end of exponential growth, the 550 nm OD was approximately 16 times that of the control flask. Note that the control flask received that same relative gas flow carbon dioxide supplementation but half the Alginator PAR intensity.

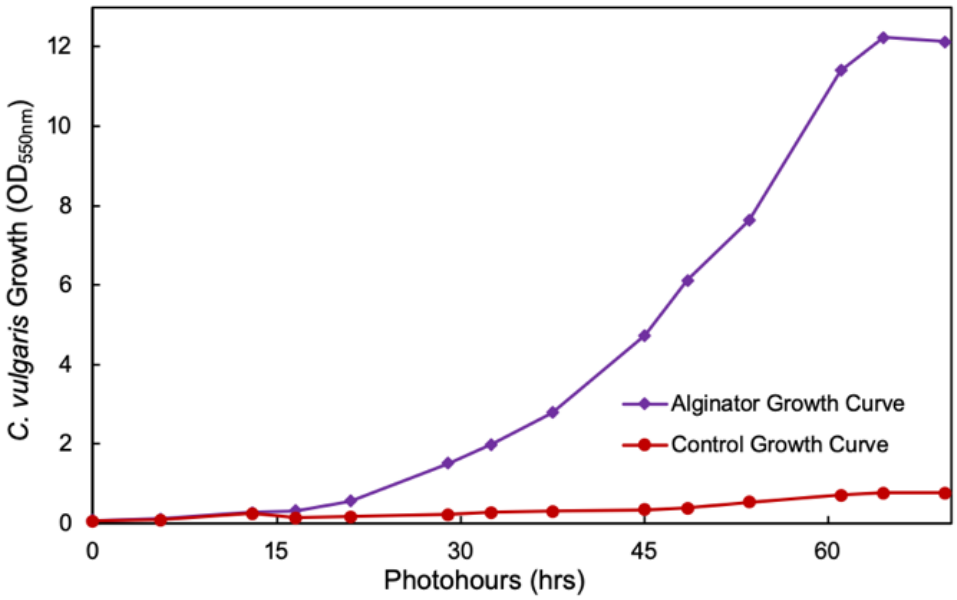

Figure 22: Growth curve at the robust optical density (OD) of 550 nm in the Alginator at 119 $\frac{\mu E}{m^2 * s}$ PAR flux versus a control flask on a shaker under PAR lighting of approximately 60 $\frac{\mu E}{m^2 * s}$.

Figure 23 analyzes the comparison on the basis of relative PAR-hours, a unit that normalizes growth based on total incident PAR light rather than time. Note that this normalization is approximated, as it accounts for differences in PAR intensity but not surface area or geometry. In fact, one of the driving principles in creating the Alginator was to have a

system that could be easily characterized for incident and absorbed PAR flux due to the difficulties in doing so with a shake flask. Applying the normalization factor, the Alginator productivity outperforms the control by a factor of 3 at the cessation of growth.

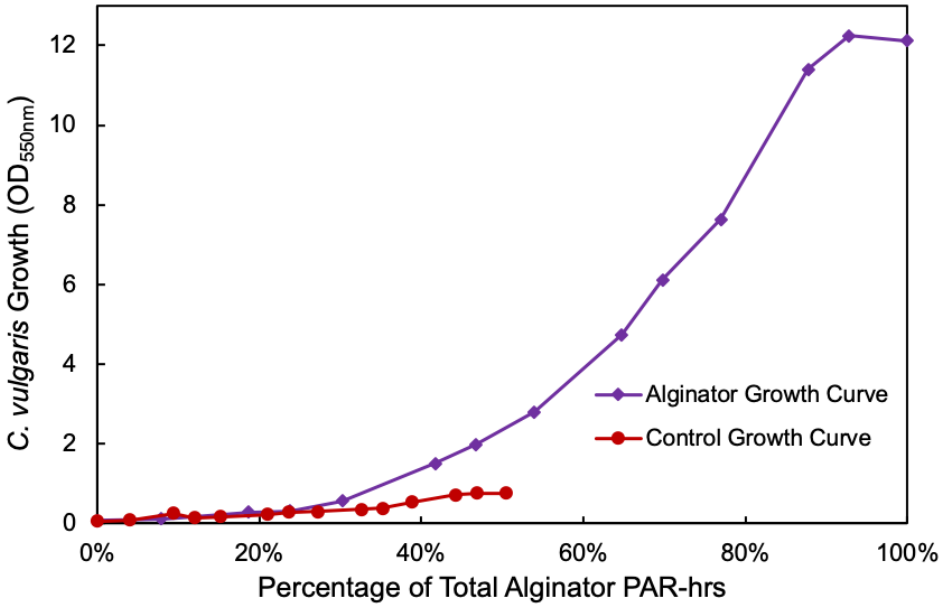

Figure 23: Comparison of Alginator versus control growth, normalized to PAR-hours to account for the difference in PAR flux.

Chapter 5

Quantification of CO_2 Mass Transfer and Carbon Limitation

In order to interpret photosynthetic efficiency (PE) during growth, it is vital to determine the limiting conditions. Photosynthetic microalgae are typically limited by carbon dioxide, nutrients, or usable (biologically accessible) light availability. The maximum PE in continuous operation is most often found when the microalgae is grown under light-limited conditions.[12] In this thesis, the culture is considered light-limited when not carbon-limited and prior to the stationary growth phase. A mass balance analysis around carbon allows determination of if the available carbon dioxide in the liquid culture was sufficient to meet the carbon dioxide uptake rate (CUR) demand. Relatedly, calculating the oxygen evolution rate (OER) throughout growth allows for understanding of the dissolved oxygen (DO) level in the culture. This is an important metric to quantify, because high DO levels have been shown to stunt photosynthetic efficiency (PE) due to the heightened occurrence of photorespiration.[30]

Stoichiometry of a photosynthetic reaction

Growth can be characterized as a 'biological reaction' to produce biomass. As discussed in Wang et al. (2016), the generalized photosynthetic reaction, with nitrate-based media like WFAMC, is,

$$\alpha CO_2 + \beta NO_3 + \chi H_2O \rightarrow CH_XO_YN_Z + \delta O_2 \qquad \textbf{Equation 3}$$

and can be used alongside measured biomass elemental composition to understand the stoichiometry of growth.[35]

Several important properties can be quantified from this analysis, and the two utilized in this study are 1) The percentage carbon of biomass, allowing for calculation of the carbon dioxide uptake rate (CUR) and 2) The photosynthetic quotient (PQ), which is the stoichiometric ratio of utilized carbon dioxide to evolved oxygen (δ/α in **Equation 3**). These analyses were performed by Wagner et al. (2006) for photosynthetic *C. vulgaris* growth in nitrate-based media, yielding 1) a 51 mass% carbon content and 2) a PQ of 1.31.[36] It is further be assessed that, on a stoichiometric basis of biomass carbon content, coefficient α for CO_2 must equal one, as there are no other carbon sources available.

These results are used throughout this first principles analysis for mass transfer and mass balance analyses; however, it is recommended for future Alginator studies that the elemental composition be measured experimentally improve accuracy. This is primarily because differences in composition and reaction stoichiometry can occur with changes to nitrogen source and growth conditions.[35,36]

Determination of the CO_2 mass transfer coefficient (k_La_{CO2})

The mass transfer of gas-phase carbon dioxide into liquid is defined using an overall mass transfer coefficient called the k_La_{CO2}. The "k_L" term represents the mass transfer coefficient of carbon dioxide and the "a" term is the total interfacial contact area between gas and liquid phases. The generalized equation for this mass transfer is,

$$\frac{dC}{dt} = k_L a_{CO2} * (C^* - C) \qquad \textbf{Equation 4}$$

where C^* is the equilibrium concentration of carbon dioxide in the system, C is the concentration of carbon dioxide, and t is time.[37] One method of enhancing mass transfer into an airlift system is to bubble gas in via a sparger, as shown in **Figure 24**. A sparger decreases the size of a bubbles, serving to enhance contact surface area "a" and allow for more consistent liquid flow.

Figure 24: Sparger inserted in the Alginator underneath the flow path to drive flow in the Alginator, supplement the culture with carbon dioxide, and enhance mass transfer by increasing the total surface area of gas-liquid interface.

There are several physical, chemical, and biological methods available for calculating the k_La_{CO2} with varying degrees of difficulty and accuracy.[37] The equilibrium between carbon dioxide and carbonic acid in solution adds complexities to calculation methods that similar calculations of oxygen mass transfer do not. In the Alginator, the k_La_{CO2} was measured over a range of gas flow rates using the pH time course method. This method takes advantage of the equilibrium dissociation of aqueous carbon dioxide into carbonic acid by measuring the change in pH over time. Several researchers, including Hill et al. (2006),[38] Sieblist et al. (2011),[39] Valdes et al. (2012),[40] and Ying et al. (2013)[41] have developed empirical correlations to determine the mass transfer coefficient in reactors via pH time course. The method for the Alginator work follows research conducted by Ying et al. (2013) in developing empirical correlations for an

airlift bioreactor with 5% carbon dioxide. Note that their method was derived using a larger (7L) internal-loop airlift reactor, however the volumetric mass transfer coefficient principles were assumed constant given circulating, microbubble-driven flow on bench-scale. The correlation of carbon dioxide to pH as derived by Ying et al. (2013) is,

$$C_{CO_2} = \frac{(10^{-pH} - 10^{pH-14}) * (10^{-2*pH})}{10^{-6.381-pH} + 2 * 10^{-16.758}} \qquad \textbf{Equation 5}$$

and was used for the Alginator mass transfer calculations. The setup used to measure the pH time course in the Alginator is shown in **Figure 25**, where a pH probe is inserted into the entrance of the downcomer to avoid the noisy effects of bubbles and the pH is read with a pH meter.

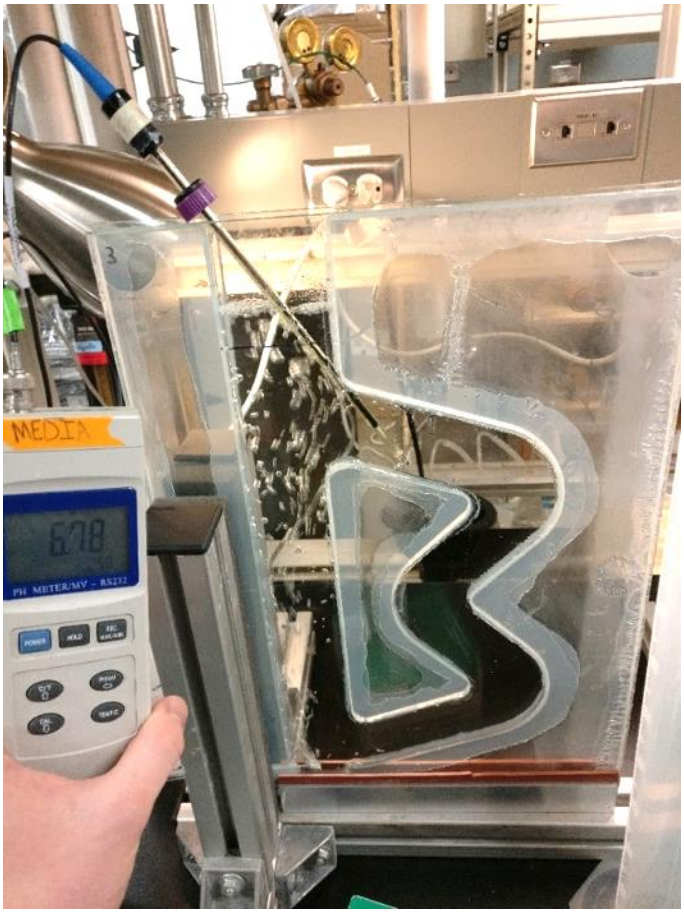

Figure 25: Setup for measurement of pH time course in the Alginator for the determination of k_La_{CO2}. A pH probe was inserted into the downcomer of the Alginator and a time course pH measurement was taken at various flow rates.

Carbon dioxide was mixed with air to a 5% carbon dioxide concentration and was bubbled into the Alginator over a range of gas flow rates**.** A timescale of 15 seconds was used for the pH measurements, beginning from a pH steady state with air and ending at steady state after carbon dioxide was introduced at 5%. Results of the experiment are shown in **Figure 26**, which display a larger and more rapid decrease in pH as vvm is increased at the constant 5% carbon dioxide concentration.

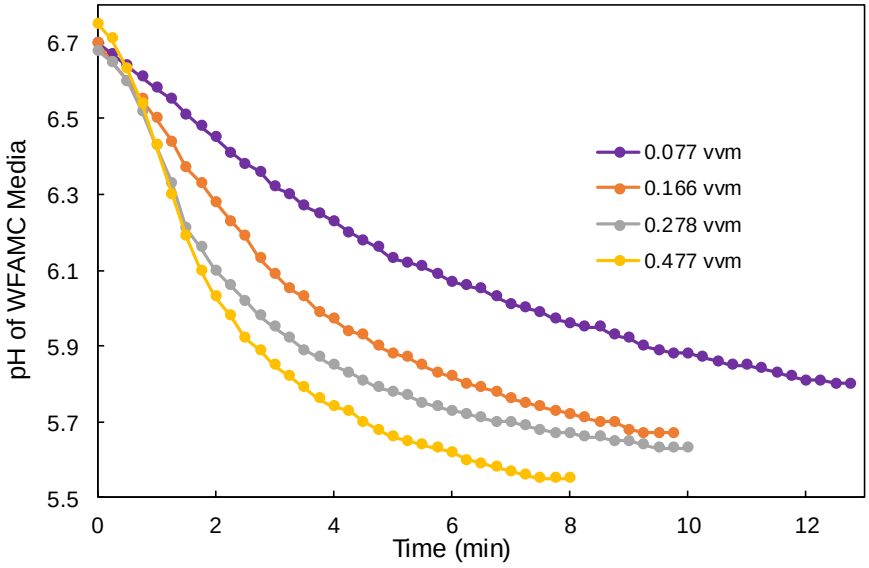

Figure 26: pH time course with 5% CO_2 in air sparged into the Alginator over a range of vvms (L/L/min).

The pH time course for each vvm was converted to concentration of carbon dioxide in liquid solution using **Equation 5**. At infinite time steady state, all vvms at 5% carbon dioxide concentration theoretically would asymptotically reach a consistent steady state pH value. Accordingly, the lowest pH achieved by the highest vvm trial was used as the C^* term for all vvms in **Equation 4**. An example result from this analysis is shown in **Figure 27**, comparing pH time course at a vvm of 0.278 relative to dissolved carbon dioxide concentration.

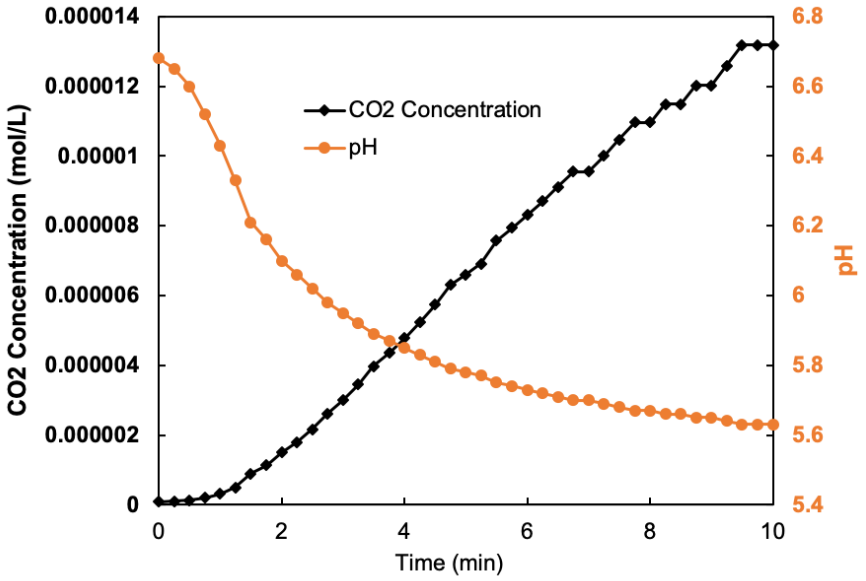

Figure 27: pH time course of 5% CO_2 in air sparged into WFAMC media in the Alginator at a vvm of 0.278, as compared with the CO_2 liquid concentration time course using **Equation 4**.

Excel was used to create a best fit regression for each concentration profile and the Solver Add-in was utilized to determine the k_La_{CO2} by least-squares regression of **Equation 4**. The final results are shown in **Figure 28**.

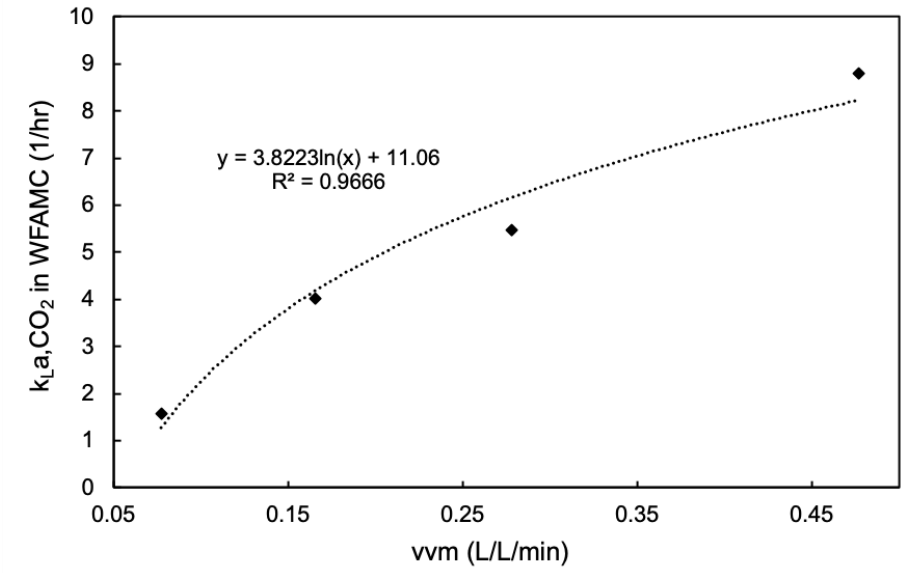

Figure 28: The overall mass transfer coefficient in the Alginator using a 5% CO_2 gas mixture into WFAMC media.

Figure 28 displays a fairly strong fit of a logarithmic correlation between gassing rate and the gas-liquid mass transfer coefficient. This correlation was used to estimate the k_La_{CO2} for the Alginator at a vvm of 0.2, yielding 4.91 1/hr. Growth of *C. vulgaris* was conducted using a 2.5% carbon dioxide gas mixture, as compared to the 5% carbon dioxide driving force from in measuring the mass transfer coefficient. Note that in the simple mass transfer definition of **Equation 4**, the interface mass transfer coefficient is not dependent on the gas composition, because the solubility of the gas in the media is captured in the driving force. Notably, Ndiaye et al. (2018) suggested that k_La_{CO2} increases with carbon dioxide concentration in a large-scale airlift PBR, however that consideration is minimally relevant to this bench-scale analysis.[42]

Characterizing CO_2 requirements

With known elemental composition of biomass and stoichiometry of photosynthetic growth, the molar carbon dioxide uptake rate (CUR) of the culture can be assessed from the observed growth rate. From the stoichiometric analysis, the carbon mass percent of *C. vulgaris* was determined to be 51%, and each mole of carbon in biomass was assumed to come from one mole of carbon dioxide. From these assumptions, the CUR was calculated throughout growth. In carbon-limited conditions, the demand for carbon will balance with the supply such that,

$$CUR = k_L a * (C^* - C) \qquad \textbf{Equation 6}$$

where CUR is in mol/L/hr, k_La is the operational overall mass transfer coefficient in 1/hr, C^* is the equilibrium liquid concentration of carbon dioxide in mol/L, and C is the concentration of carbon dioxide in bulk solution in mol/L.

Equation 6 represents a balance of the available capacity for mass transfer (k_La) and the driving force necessary to achieve the observed mass transfer rate. The utility of this relationship is that it allows one to examines the constraints this represents on growth rate. The maximum mass transfer rate will occur when the driving force is the greatest – when the dissolved carbon dioxide (C in **Equation 6**) is being utilized so rapidly that it is pulled close to zero in solution.

An alternative perspective is that one can calculate the minimum k_La that is needed to supply an observed carbon uptake rate,

$$CUR = k_L a, min * (C^*) \qquad \textbf{Equation 7}$$

where the observed CUR should be less than or equal to the $k_La_{,min}$ required at the maximum driving force. In essence, by combining the observed growth rate with the stoichiometry of carbon incorporation into biomass, one can then calculate the minimum mass transfer coefficient that is needed to supply that carbon dioxide transfer rate at the operational carbon dioxide composition of the bioreactor.

The C^* value in **Equation 7** was calculated using the Henry's Law equation,

$$C^* = \frac{y_{CO_2} * P_{avg}}{H} \qquad \textbf{Equation 8}$$

where y_{CO2} is the mole fraction of carbon dioxide, P_{avg} is the average pressure in the system, and H is the Henry's Law coefficient.[43] WFAMC was approximated as water in these calculations, as literature has shown little deviation Henry's Law coefficient values between water and algal media.[41] The Henry's Law coefficient for carbon dioxide in water is approximately 26.6 L*atm/mol at 22˚C.[44] The average operating pressure of the Alginator is dictated by,

$$P_{avg} = \rho g h_{avg} \qquad \textbf{Equation 9}$$

where g is the gravitational acceleration, ρ is the density of water, and h is the height of the liquid head. The maximum height of the liquid head was measured as 0.35 m, such that the average height of the flow path was at half this height, 0.18 m. The calculated average pressure for the system was thus calculated as 1.02 atm. Tescione et al. (1999) concluded that using average pressure for equilibrium calculations is accurate for a well-mixed liquid phase.[45]

Figure 29 compares the Alginator experimental k_La_{CO2} of 4.91 1/hr at the operational 0.2 vvm as compared to a time course of $k_La_{,min}$ as calculated using the observed CUR. The red line represents the minimum mass transfer needs at the experimental 2.5% carbon dioxide concentration and 0.2 vvm throughout the *C. vulgaris* growth curve and the purple line represents theoretical $k_La_{,min}$ values if the culture were grown with 5% carbon dioxide supplementation. The green line represents the calculated Alginator k_La_{CO2} of 4.91 1/hr.

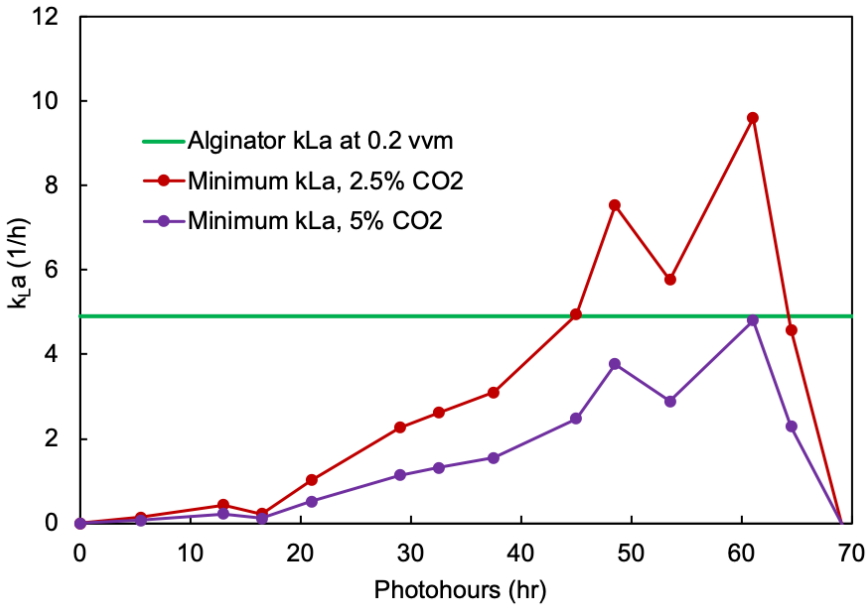

Figure 29: Alginator calculated k_La_{CO2} and minimum k_La throughout the growth curve. The $kLa_{,min}$ crosses the experimental kLa_{CO2} value, implying that the culture may have experienced carbon-limited growth at the highest growth rates. The theoretical 5% CO2 case is also shown, lying below the k_La_{CO2} value at all times.

The analysis shows that towards the end of the growth curve, when specific growth rates and cell concentrations are highest, the carbon demand is approaching or reaching the maximum possible supply provided by $k_La_{,min}$. As this occurs, the condition of growth may have been limited by carbon rather than light. This observation does not alter the ability to measure photosynthetic efficiency (PE), but it may alter interpretation and how these efficiencies may translate to a larger scale reactor. As noted in my previous discussion, full scale algae bioreactors will be light limited, therefore it is desirable to assess the implications of this observation on the proposed use of the Alginator for PE assessments.

Note that the actual $k_La_{,min}$ can only ever get as high as equaling the k_La_{CO2}, because a value higher represents a growth condition out of carbon mass balance. This result indicates that one or several of the following things occurred: 1) the calculated k_La_{CO2} value is lower than actuality based on the empirical correlation, 2) the $k_La_{,min}$ values are higher than actuality, and/or 3) the culture was limited by carbon for some portion of growth. Regardless of the source of error, there are several changes that can be made to ensure the culture maintains light-limited conditions. These changes can take place in future experiments to decrease uncertainty and ensure light limitation throughout the entirety of growth, and include:

1. **Earlier culture harvest:** One solution would be to harvest the microalgae prior to the point at which carbon limitation is expected to take place, such the analysis only considers efficiency during light limited conditions. This may involve selecting a maximum OD level or growth rate at which to cease growth and harvest.
2. **Increase CO_2 supplementation:** Huang et al. (2017) suggested that up to 5% carbon dioxide could be utilized without achieving toxic pH levels.[30]As plotted in **Figure 29**, a 5% carbon dioxide concentration would have kept the culture from ever reaching carbon limitation, so it is recommended that future studies increase carbon dioxide concentration to this level. Future experiments could also use certain biomass growth rates as triggers to increase the CO_2 supplementation to avoid the carbon limitation zone.

3. **Validate calculated k_La_{CO2}:** A secondary technique should be used to remeasure and verify the experimental k_La_{CO2} value obtained. One approach is to avoid the complexity of CO_2 and measure the oxygen mass transfer by dynamic aeration or sulfite oxidation – and then adjust the k_La based on the ratio of the CO_2 and O_2 diffusion coefficients in the interface boundary layer.[38]
4. **Increase accuracy of $k_La_{,min}$ values:** More frequent or continuous measurement of OD would limit the calculation impacts of minor errors in OD and improve overall accuracy and understanding of the growth curve. Myers et al. (2013) investigated an LED/photodiode flow cell that could potentially be modified for this purpose.[32]

Dissolved oxygen (DO) analysis

Simultaneously with the uptake of carbon dioxide into the culture, microalgae release oxygen as a product of photosynthetic growth. It is important to understand the dissolved oxygen (DO) level in the culture throughout growth, as a higher partial pressure of oxygen leads to a higher incidence of photorespiration and possible decline in light capture efficiency.[30] Production of oxygen is measured as the oxygen evolution rate (OER) and is directly related to the carbon dioxide uptake rate (CUR). The molar ratio of evolved oxygen to utilized carbon (OER/CUR) is known as the photosynthetic quotient (PQ) and varies by organism, growth conditions, and nitrogen source. From the prior stoichiometry discussion, the PQ for photosynthetically grown *C. vulgaris* in nitrate-based media has been calculated as 1.31.[36] Thus, the OER was determined throughout growth by multiplying the CUR by the PQ.

Assuming pseudo-steady state for dissolved oxygen (DO), OER can be represented by,

$$OER = -k_L a_{O2} * (C^* - C) \qquad \textbf{Equation 10}$$

where k_La_{O2} is the overall mass transfer coefficient, C^* is the liquid oxygen concentration at air saturation (with 21% O_2), and C is the actual liquid oxygen concentration.[46] At the average pressure calculated in Alginator operation, C^* was calculated as 0.277 mmol/L using a Henry's

Law coefficient for oxygen in water of 770 L*atm/mol.[47] Inlet oxygen in the sparged gas is slightly lower than the percentage in air due to carbon dioxide enrichment, and the exit gas is expected to be slightly higher than air due to oxygen stripping. Hence, the air saturation value was considered a reasonable average C^*. The k_La_{O2} can be calculated from the known k_La_{CO2} using the ratio of square root of diffusion coefficients of the molecules. Using this method, Liu et al. (2019) determined the correction factor from k_La_{CO2} to k_La_{O2} to be 1.05, yielding a k_La_{O2} of 5.17 1/hr from the calculated k_La_{CO2} of 4.91 1/hr.[48] The concentration (DO) was plotted against photohours in **Figure 30** as a percentage of the air saturation value.

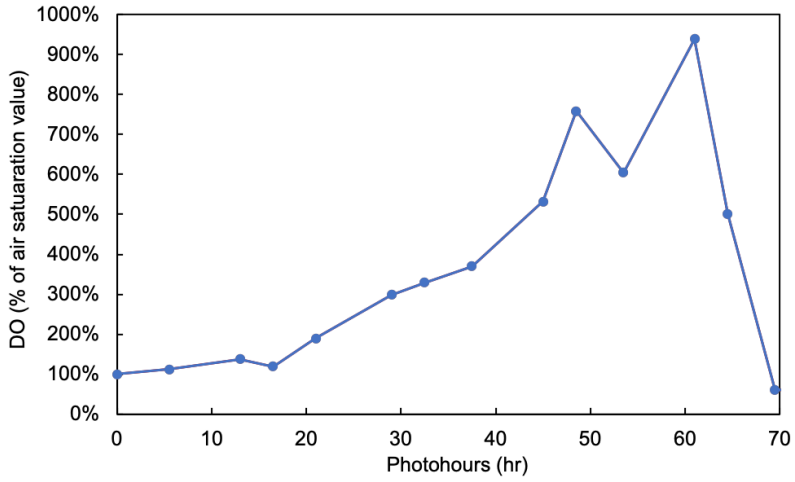

Figure 30: Time course dissolved oxygen (DO) levels during *C. vulgaris* growth in the Alginator. Regions above 476% DO represent saturation higher than pure oxygen, where the oxygen likely desorbed into the gas phase.

This analysis shows that the DO level was held significantly higher than the air saturation equilibrium for a majority of growth. Note that a 476% DO relative to air represents the equilibrium concentration of water with pure oxygen, so the DO cannot physically surpass this limit. Calculated DOs above this threshold indicate that, likely, oxygen desorbed from solution and formed bubbles. These results indicate that DO may play a significant role in the growth dynamics and efficiency of Alginator. Steps such as decreasing oxygen percentage in the inlet gas and operating at a higher k_La_{O2} could help optimize future growth conditions.

Chapter 6

Energy Balance as Photosynthetic Efficiency (PE)

Determining chemical energy produced as biomass

Bomb calorimetry was used to determine the amount of chemical energy produced in the Alginator as biomass. To prepare the sample, the harvested liquid sample was centrifuged at 3500 rpm for 8 minutes to separate the solid algae cells from the supernatant. The sample was then dried in a 70 ˚C oven overnight. Finally, the dried sample was pelletized using a pellet press into samples of 1.5 mg. Notably, the algae was not harvested until 80.5 photohours, approximately 20 photohours after the end of exponential growth. Under the nitrogen-starved stationary phase, *C. vulgaris* can accumulate lipids. The harvested biomass composition was considered the average composition for this work, however future experiments are recommended to harvest the algae as soon as the stationary phase is predicted to begin or even during the late exponential growth phase to avoid this possible discrepancy.

Energy density of *C. vulgaris* was determined using triplicate measurements on a bomb calorimeter (Parr 6200) with benzoic acid as calibration. Visual depictions of the bomb calorimetry method used can be seen in **Figure 31.** The resulting energy density calculated of *C. vulgaris* harvested from Alginator was 19.0 ± 0.2 kJ/g biomass. This relationship was used alongside mass growth rate to calculate the time course chemical energy produced as biomass.

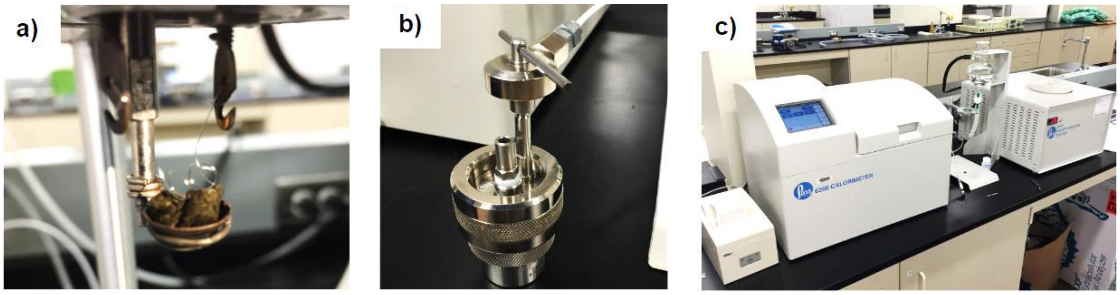

Figure 31: a) Loading of dried *C. vulgaris* sample. b) Adding oxygen to bomb. c) Parr 6200 bomb calorimeter used.

Determining the biologically accessible photon (BAP) energy

In this analysis, only light energy as photosynthetically active radiation (PAR) photons absorbed by the culture was considered in the photosynthetic efficiency (PE) calculations. This approach omits the light that passes completely through the culture and hence yields the biologically accessible photons (BAP). This approach thereby focuses on the intrinsic efficiency of the organism by filtering out differences of lighting sources as well as size and geometry of PBR when comparing results between studies. In this context, the value of the Alginator design reflects its intended purpose for screening algae that have intrinsically higher photon use efficiency, which is suggested to be more important than intrinsic rate of growth for translation to large scale bioreactor performance.

To calculate the incident photon energy, the emission spectrum of a linear tube 3500K fluorescent bulb was adapted from an analysis performed by Soleymani et al. (2017).[49] Their analysis measured the emission spectrum of a linear tube 3500K fluorescent bulb 15 cm from a measurement point.[49] This was assumed to be approximetly equivalent to the 3500K fluorescent bulb illuminating the Alginator from an 18 cm distance on each side. **Figure 32** shows this spectrum with normalized power intensity, digitized with the use of the open-source Plot

Digitizer 2018 software found at the following link, as develoepd by user 'jhuwaldt': https://sourceforge.net/projects/plotdigitizer/. Within the PAR-spectrum range (400-700 nm), the integral as calculated in Excel yielded an average wavelength of 542.8 nm based on photon wavelength-dependent power.

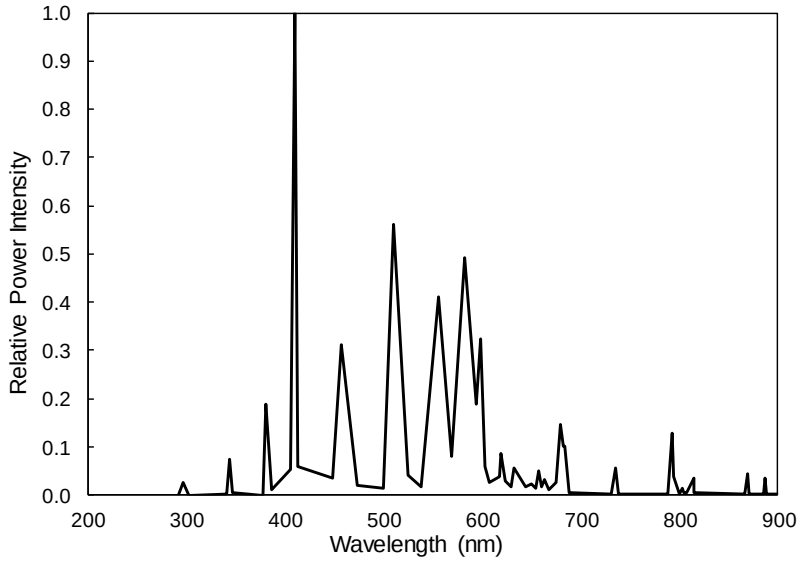

Figure 32: Adapted from the fluorescent light spectrum of a 3500K bulb as measured by Soleymani et al. (2017).[49] The average wavelength based on photon wavelength-dependent power was calculated as 542.8 nm within the PAR range.

Planck's equation gives the energy of a photon at a certain wavelength,

$$E = \frac{hcA}{\lambda} \qquad \textbf{Equation 11}$$

where E is the energy per mole photon, c is the speed of light, A is Avogadro's number, h is Planck's constant, and λ is wavelength. The speed of light was taken as 299,792,485 m/s, Planck's constant as $6.626*10^{-34}$ m^2*kg/s, and Avogadro's number as $6.0221*10^{23}$ 1/mol. **Figure 33** was developed by calculating the energy per mole photon by wavelength throughout the PAR range. The resulting average PAR photon energy density was 220.4 kJ/mol for the spectrum in **Figure 32** using the average wavelength of 542.8 nm.

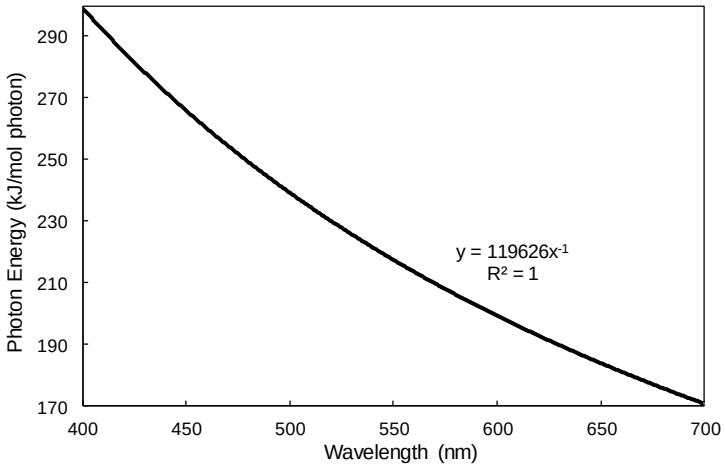

Figure 33: Photon energy per mole photons versus photon wavelength. The calculated average energy of the incident light to the Alginator was 220 kJ/mol at 542.8 nm.

Recall that one of the two light racks was off for the first 16.5 photohours of growth with both racks used for the remainder of growth afterwards. The incident PAR photon flux was thus calculated as 0.0181 mol/photohour for the first 16.5 photohours and 0.0362 mol/photohour afterwards, due to the effective doubling of illuminated surface area at the same PAR flux intensity.

The Beer-Lambert Law was used to determine a correction factor to account for the photons transmitted through the system. The photons transmitted through were omitted in the BAP analysis because they were not absorbed by the liquid culture and could thus not be used in photosynthesis. The Beer-Lambert law is described by,

$$A = \epsilon c l = \log_{10} \frac{I_0}{I} = -\log_{10} T \qquad \textbf{Equation 12}$$

where A is absorbance, ε is the absorption coefficient, c is concentration, l is the optical path length, I_0 is the incident light, I is the transmitted light, and T is the fractional transmittance of light.[50] The incident light I_0 into the Alginator was $119 \pm 3 \frac{\mu E}{m^2 s}$ PAR flux. The transmitted light, I, is far too small at high culture densities to be measured within a reasonable range. Thus, a

calculation was developed to approximate PAR absorbance using the ODs measured at 550 and 680 nm during growth.

From the Beer-Lambert Law, **Figure 34** shows the modeled total PAR flux through the Alginator light path at a variety of ODs observed during growth. The cases where one rack was illuminated (until 16.5 photohours) and where both racks were illuminated (after 16.5 photohours) are shown for comparison. This visualization also displays that there exists a dark region in the center of the light path for the highest ODs, where photosynthesis cannot occur. Hence one more reason why adequate mixing is necessary in the Alginator, for keeping all algal cells circulating into the illuminated zone without extended time in the dark region.

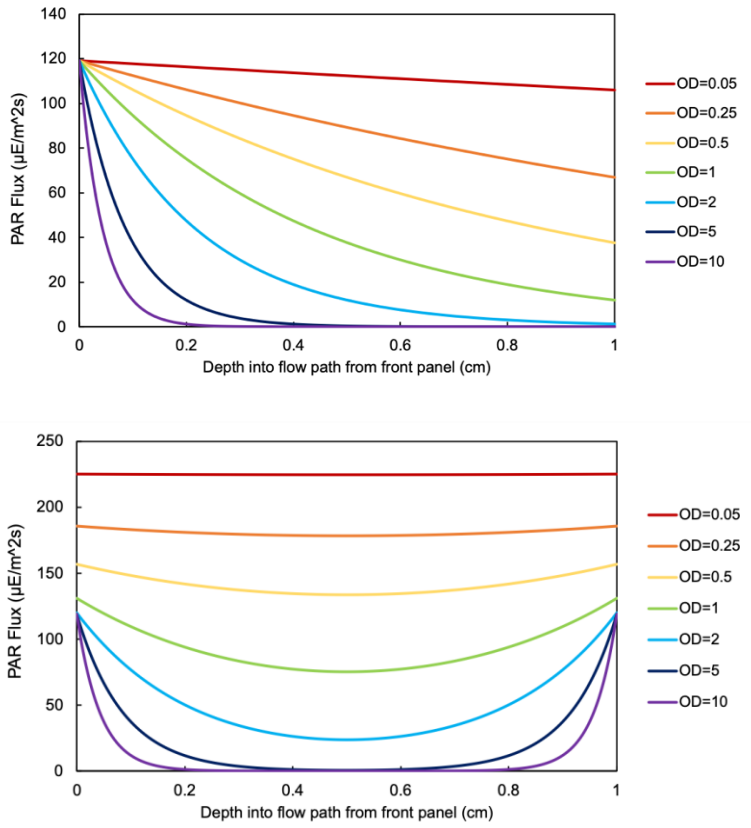

Figure 34: Top: Visualization of PAR photon flux through the light path of the Alginator at a variety of ODs with one light rack illuminated versus Bottom: with both light racks illuminated.

Myers et al. (2013) measured the absorption spectra of *C. vulgaris*, and normalized the spectra to the robust optical density of 550 nm as shown in **Figure 35**.[32] The most rigorous method of determining PAR absorbance at each OD is to measure the PAR spectrum absorbance for each sample. Since the spectrophotometer cuvette and the light path length of the Alginator are both 1.0 cm, OD can be approximated as absorbance in the Beer-Lambert Law (**Equation 12**). The absorbance spectrum in the PAR range can then be overlaid with the light emission spectrum. **Figure 35** shows a rigorously calculated example, using the 2.09 OD550 measurement by Myers et al. (2013) and the fluorescent spectrum in **Figure 32**. The integral of the emission spectrum in the PAR range was normalized to the total PAR flux, yielding the relative photon flux at each wavelength. The addition of relative fluxes allows for calculation of total PAR absorbance. In the given example, the resulting total PAR absorbance was 2.42.

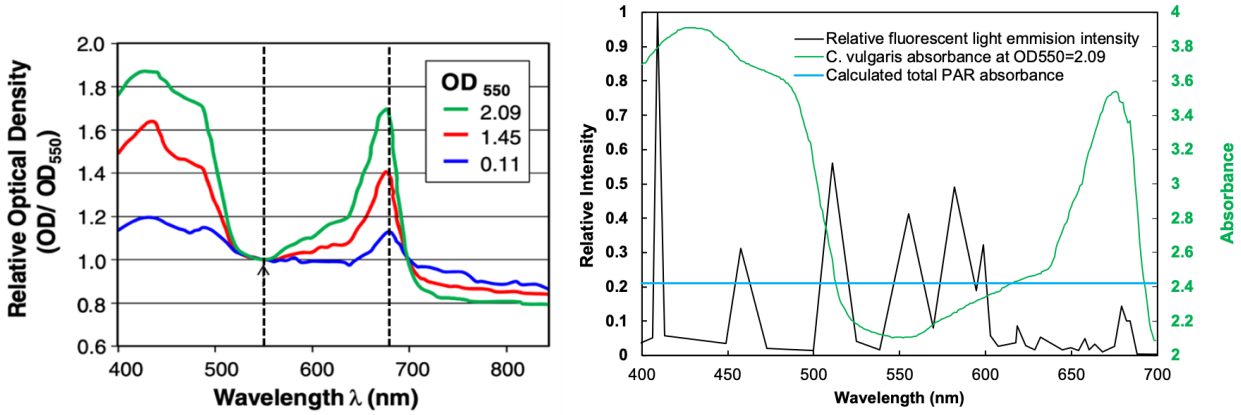

Figure 35: Left: Adapted from Myers et al. (2013). Absorption spectra of *C. vulgaris* measured at three undiluted concentrations and then normalized to the robust optical density at 550 nm.[32] The dashed lines represent the two wavelengths, 550 nm and 680 nm, measured for *C. vulgaris* growth in the Alginator. Right: Overlay of fluorescent light emission spectrum from **Figure 32** and literature *C. vulgaris* absorption spectrum at OD550=2.09 shown left. The blue line shows the resulting PAR absorbance of 2.42.

It is evident that the total PAR absorption, calculated here as 2.42, is between the OD 550 nm value (2.09) and 680 nm value (3.48). This trend is expected throughout the entirety of growth, because the robust 550 nm measurement is dominated by light scattering and produces a

relative minimum, while the 680 nm measurement represents the maximal absorption. Hence, with these as boundaries, the average of the two values was used to determine the BAP.

From **Equation 12**, the absorbance (as average OD) was used to determine the BAP. The resulting time course BAP in comparison to average OD is shown in **Figure 36**. Note the large spike in BAP after 16.5 photohours, when the second rack of lights was turned on. Important to note as well is that BAP remain nearly constant at OD measurements higher than 2, where one could reasonably estimate efficiency from incident PAR due to the negligible amount of light transmitting through the culture. This is because an OD of 2 represents 99% of the incident photons absorbed, and values higher represent asymptotically approaching 100%.

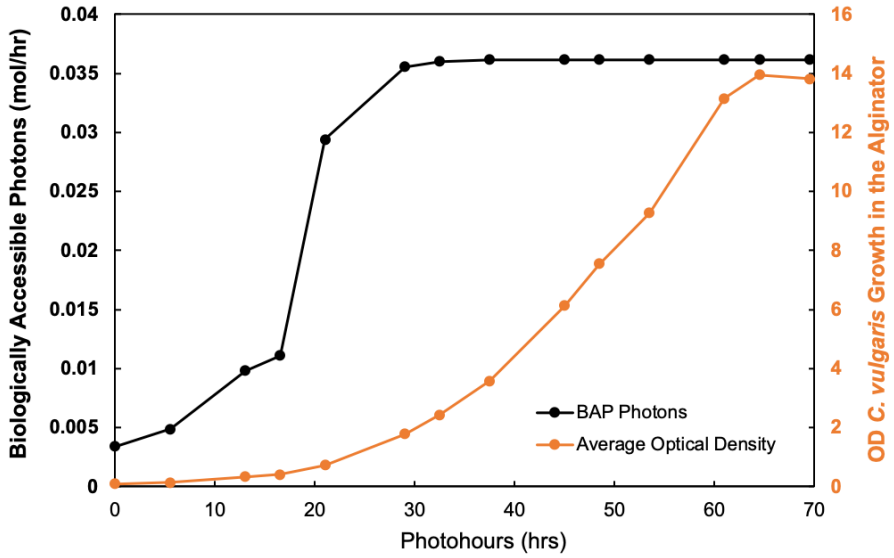

Figure 36: Biologically accessible photon (BAP) analysis into the Alginator, compared to the averaged OD from 550 nm and 680 nm measurements. Only one set of lights was on during daylight hours for the first 16.5 photo hours of growth, accounting for the large spike when full light is implemented.

BAP PE results and discussion

PE results

The energy balance on growth is represented as PE in this analysis as a simple percentage of the chemical output energy from biomass over the light energy input as BAP. Biomass chemical energy output was calculated as a product of energy density (bomb calorimetry) measurements and biomass growth as determined by optical density (OD). Light energy input was determined using the BAP profile in **Figure 36** with the calculated PAR photon energy of 220.4 kJ/mol. The resulting PE is graphed in **Figure 37**.

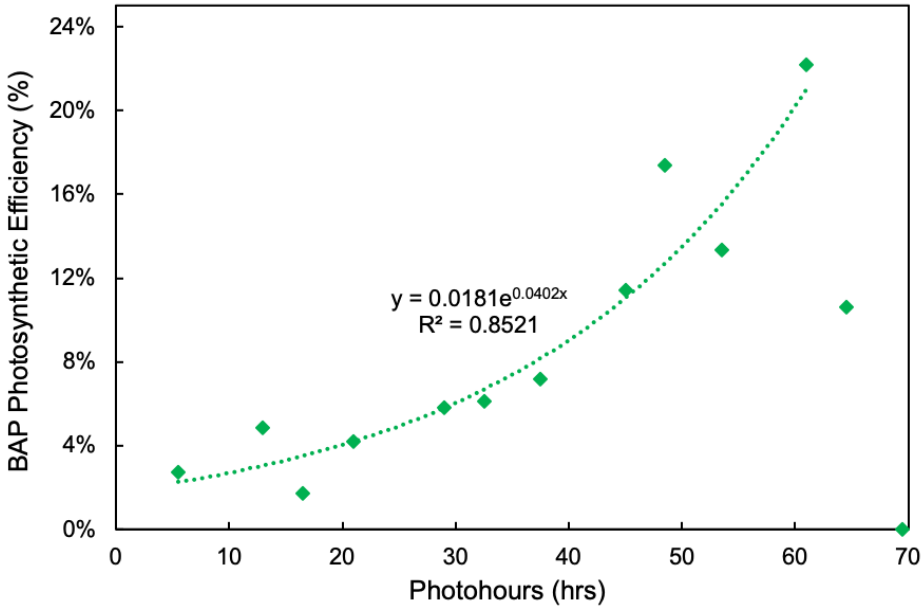

Figure 37: Time course of photosynthetic efficiency (PE) expressed in photohours of *C. vulgaris* in the Alginator. The maximum calculated PE is 22.0% at 61 photo hours. Variability in the calculated PE values show the sensitivity of the PE calculations to minor measurement error in mass growth rate.

The maximum BAP photosynthetic efficiency (PE) for *C. vulgaris* growth in the Alginator was 22% as calculated at 61 photohours. The average BAP PE during the exponential growth phase from inoculation to 61 photohours was 8.8%. The trend of BAP PE follows a

power law function until approximately 61 photohours where exponential growth stops, and stationary growth begins.

Note the exponential fit presented only accounts for inoculation until 61 photohours, at which time the culture was assumed to be nutrient limited. The deviations from a smooth trend are likely due to derivative rate calculations from slight measurement error in OD, introducing a degree of uncertainty in the PE analysis. One mitigation technique would be a continuous OD measurement. The LED/photodiode flow cell developed by Myers et al. (2013) could potentially be modified for this purpose.[32] Another strategy to solve this could be a PAR sensor for continuous measurement of absorption through the light path, however, as noted in the BAP calculations, the nature of OD measurements as transmitted light would greatly reduce this accuracy unless there was an accommodation for a smaller path length. This adjustment could be accomplished with an acrylic 'light guide' that would span part of the light path.

PE discussion

As established in the Tuerk and Grady theses, intrinsic growth rate is a poor indicator of PE or solar-to-biomass energy conversion to use in the evaluation of algae biofuels candidates.[12,13] Specifically, their work demonstrated that *B. braunii* could out-produce *C. vulgaris* energetically four-fold despite a doubling time of 2-3 days in comparison to *C. vulgaris'* 3-6 hours. Furthermore, they demonstrated the critical nature of measuring algae biofuels candidates' performance under relevant operating conditions; namely, by emphasizing the importance of light-limited conditions and continuous operation.

Evaluation of candidates by intrinsic growth rate or productivity when energy potential is not light limited such as when grown under (1) nutrient limitation, (2) rate limitation by poor carbon mass transfer, or (3) poor reactor design limiting light penetration is a fundamentally flawed criterion. Rather, calculated maximum PE is the best indicator of intrinsic performance potential because it characterizes energetic productivity by providing a 'snapshot' of productivity that can be maintained at steady-state under light-limited, high-density, continuous operation. In essence, PE answers not which algae can grow the fastest but which algae can most reliably convert the available light energy efficiently. Note that as discussed in Chapter 5, adjustments should made in future Alginator work to ensure that the maximum calculated value of PE is made under light limited conditions.

Models for microalgae growth generally state that BAP PE should not surpass the 27-29% range.[51,18] A reported BAP PE above the 27-29% range would indicate a likely error in the measurement or calculation methods of the Alginator work. The maximum observed PAR PE in the Alginator was 22% which is below this threshold and is therefore a plausible maximum.

Nwoba et al. (2019) produced a study comparing experimental microalgae PE values calculated using a variety of strains, growth conditions, and types of outdoor sunlit photobioreactors.[7] The study suggested that the experimental PE values for microalgae ranged from 0.5 to 16% across a broad survey of microalgae energy balance results. However, the study also showcased the challenges in comparing PE values for a given microalgae species. For example, the calculated PE for the strain *Nannocloropsis sp.* varied in the study from 0.5% to 8% depending on reactor volume, reactor geometry, and light conditions. This large difference in calculated PE within the same species highlights the need for consistency in PE conditions and assumptions for comparison. Similar conclusions were reached in a study by Kula et al. (2014)

that describes inconsistencies in variable definitions and growth conditions as hindering the ability to usefully interpret PE results.[52] This difficulty is one reason that many researchers choose to report more straightforward parameters such as biomass productivity rate instead.[33,53]

Specifically for *C. vulgaris*, research was conducted by Fu et al. (2012) under light-limited conditions and only including PAR-spectrum light in the PE analysis.[33] Light was provided at 660 nm from an LED and gas was introduced at 2.5% carbon dioxide by volume. The maximum yield reported in the work by Fu et al. (2012) was 0.88 g biomass/mol photons.[33] Using the energy density and light energy correlations from the Alginator work, the PE from the Fu et al. (2012) was calculated as 9.0% over the three-day growth period. The average PE value obtained over the growth period of *C. vulgaris* in the Alginator was 8.8%, suggesting that the Alginator value reported is reasonable in relation to literature values with similar conditions. This also stresses the reproducibility with which algae candidates can be evaluated when grown with consistent conditions and assumptions, despite different bioreactor designs.

Chapter 7

Key Conclusions and Future Work

Key Conclusions

The Alginator, a bench-scale, flat-panel external-loop airlift photobioreactor (PBR), was preliminarily validated as a platform for robust microalgae characterization by photosynthetic efficiency (PE). While there are some improvements that could be made to minimize assumptions within this validation, the Alginator was generally confirmed to (1) be well-mixed, (2) support high mass transfer, (3) support light-limited growth, (4) enable closure of energy balance, and (5) reproduce previously reported values of photosynthetic efficiency for *C. vulgaris*. Utilized correctly, the work of this thesis can be a backbone for quick and accurate comparison of microalgae for PBR characterization and a starting point for assessment of feedstock selection.

The fluid dynamics in the Alginator were characterized, and flow was confirmed to be well-mixed throughout the experimental range. At the experimental conditions of 0.2 vvm and 2.5% carbon dioxide by volume, the k_La_{CO2} was determined to be 4.91 1/hr. From the calculations of carbon inputs (derived from mass transfer rate) and outputs (product of biomass growth and assumed carbon content), a subsequent mass balance analysis around carbon determined growth to be light limited except possibly at the highest growth rates. Analysis of dissolved oxygen indicated near or at oxygen saturation conditions throughout a majority of growth. Bomb calorimetry was used to determine the energy density of harvested *C. vulgaris*, yielding 19.0 ± 0.2 kJ/g biomass. The maximum biologically accessible photon (BAP) photosynthetic efficiency (PE) of *C. vulgaris* measured was 22%, with an average PE of 8.8%

during the exponential growth phase. The maximum calculated PE was considered reasonable given current models that yield a maximum theoretical PE value of 27-29% with PAR photons.[18,51] Calculation of average BAP PE for *C. vulgaris* over the course of growth is typically reported around 9%, corroborating the Alginator results.[33,7]

Future Work

Improvements to validation studies

Several improvements could be made to improve accuracy in the validation study of the Alginator, based on the learnings gleaned from this first principles analyis. All improvements are sufficiently minor, however, that none are assumed to fundamentally change the outcomes reported. The highest priority improvement is to re-verify the carbon mass transfer analysis to ensure carbon limitation is prevented. Measuring elemental composition of the harvested biomass will be vital for comparing PE of different microalgae and for ensuring light limitation. Additionally, carbon dioxide concentration of gas into the Alginator may need to be increased from the 2.5% used in this experiment up to 5%, given the rapid growth rate at high ODs.

Secondary priority improvements would be to change the frequency of sampling and timing of harvesting. A key learning from this work is that PE is very sensitive to errors in OD measurement. Mitigating this error could be done by sampling at a higher frequency, where for instance samples could be taken every photohour of growth rather than every several photohours. Ultimately, this issue could be solved by developing a continuous OD measurement method, such as the acrylic LED light guide utilized by Myers et. al (2013).[32] Regarding harvesting

timing, the sample could be harvested at or prior to the peak of exponential growth, rather than rather than several hours into the stationary growth phase. For microalgae like *C. vulgaris*, in which lipid accumulation can be enhanced by nutrient starvation, this earlier harvest would ensure that the measured energy density and biomass composition are more representative of conditions throughout the experimental growth period.

Furthering Alginator usage and adoption

The most significant future work for the Alginator is in promoting its technical adoption by the algae biofuels community. Accessibility could be achieved through research to replace the acrylic/glass panels with an open-source 3D-printed design. This would favor ease of construction but require research on thermoplastics resins that are biocompatible for algae growth and favorable in light penetration properties. Accordingly, associated light studies would need to be repeated.

Despite the introduction of the pilot-scale trickle-film reactor published nearly a decade ago, the algae biofuels community has been slow to recognize the implications; namely, the rationale provided by process engineering that intrinsic growth rate does not predict steady-state growth rate and maximized energy output. In turn, the imperative for a platform like the Alginator for robust characterization of microalgae biofuels candidates has been largely ignored. Adoption of this platform would need to be approached through (1) scientific communication of this imperative and the Alginator's design significance, (2) design optimization for ease of use, and (3) accessibility via a low-cost, open-source design. Towards this goal, the open-source CAD model for the Alginator is linked in Chapter 2 to be utilized as needed.

Appendix A

Miscellaneous Figures

Wayne's Freshwater Algae Medium for Chlorella (**WFAMC**)

Autoclave all 3 solutions separately to prevent precipitation (Ca/Mg solutions can also be filter-sterilized) and combine aseptically. Solutions can be stored at room temperature after autoclaving.
Shaded items are alternative permutations for chemical addition DO NOT ADD BOTH

	MW	[final]	[stock]	prep / L	/ 250 mL
KNO_3	101.11	2.2 g/L	--	**2.2 g**	0.55 g
MR26 Phosphates* (50x, 1M) (pH 6.8)				**1.3 mL**	0.325 mL
K_2HPO_4 (dibasic)	174.18	149.5 mg/L	115 g/L		
KH_2PO_4 (monobasic)	136.09	58.3 mg/L	44.9 g/L		
WFAM MICROnutrients (1000x)				**1 mL**	0.25 mL
H_3BO_3 (boric acid)	61.83		1.86 g/L		
$MnCl_2 \cdot 4H_20$	197.41		0.54 g/L		
$ZnSO_4 \cdot 7H_20$	287.56		0.066 g/L		
$ZnSO_4 \cdot H_20$	179		0.0411 g/L		
$ZnSO_4$ (anhydrous)	161.47		0.0371 g/L		
Na_2MoO_4-$2H_2O$	241.95		0.031 g/L		
$(NH_4)_6Mo_7O_{24} \cdot 4H_20$	1235.86		0.0229 g/L		
$CoCl_2 \cdot 6H_20$	237.93		0.030 g/L		
$CuSO_4 \cdot 5H_20$	249.7		0.0075 g/L		
Fe-EDTA$\cdot 2H_20$ (F)	403.1	2.4 mg/L	4 g/L	**6 mL**	1.5 mL
EDTA Ferric Sodium Salt	367.1	22.0 mg/L	3.67 g/L		
Fe-EDTA$\cdot 2.5H_20$	412.1	24.70 mg/L	4.12 g/L		
Fe-EDTA$\cdot 3H_20$	421.1	25.26 mg/L	4.21 g/L		

Autoclave Separately

Magnesium Solution (1M, filter sterilized)			/ 50mL stock	**1 mL**	0.25 mL
$Mg(NO_3)_2 \cdot 6H_2O$	256.41	132 mg/L	6.6 g		
$MgSO_4 \cdot 7H_2O$	246.5	121 mg/L	6.03 g		
$MgSO_4$ (anhydrous)	120.0	58.8 mg/L	2.94 g		

Autoclave Separately

Calcium Solution (1M, filter sterilized)			/ 50mL stock	**0.088 mL**	0.022 mL
$CaCl_2 \cdot 2H_2O$	147	13.2 mg/L	7.5 g		
$CaCl_2$ (anhydrous)	111	10.0 mg/L	5.66 g		
$CaCl_2 \cdot 2H_20$	147	13.2 mg/L	0.75 g	0.88 mL	0.22 mL
$CaCl_2$ (anhydrous)	111	10.0 mg/L	0.566 g		

* pH to 6.8 with KOH or H_3PO_4

Figure 38: WFAMC media formulation used in the Alginator experiments.

BIBLIOGRAPHY

1. Ruane, J., Sonnino, A. & Agostini, A. Bioenergy and the potential contribution of agricultural biotechnologies in developing countries. *Biomass and Bioenergy* **34**, 1427–1439 (2010).
2. Scherholz, M. L. Achieving ph control through Stoichiometrically balanced media in Algal photobioreactors. (Pennsylvania State University, 2012).
3. Oliphant, A. J. & Stoy, P. C. An Evaluation of Semiempirical Models for Partitioning Photosynthetically Active Radiation Into Diffuse and Direct Beam Components. *J. Geophys. Res. Biogeosciences* **123**, 889–901 (2018).
4. Vassilev, S. V. & Vassileva, C. G. Composition, properties and challenges of algae biomass for biofuel application: An overview. *Fuel* **181**, 1–33 (2016).
5. Vassilev, S. V, Baxter, D., Andersen, L. K. & Vassileva, C. G. An overview of the composition and application of biomass ash. Part 1. Phase-mineral and chemical composition and classification. *Fuel* 40–76 (2013). doi:10.1016/j.fuel.2012.09.041
6. Slade, R. & Bauen, A. Micro-algae cultivation for biofuels: Cost, energy balance, environmental impacts and future prospects. *Biomass and Bioenergy* **53**, 29–38 (2013).
7. Nwoba, E. G., Parlevliet, D. A., Laird, D. W., Alameh, K. & Moheimani, N. R. Light management technologies for increasing algal photobioreactor efficiency. *Algal Research* **39**, 101433 (2019).
8. Barry, A., Wolfe, A., English, C., Ruddick, C. & Lambert, D. *2016 National Algal Biofuels Technology Review*. (2016).
9. Sun, A. *et al.* Comparative cost analysis of algal oil production for biofuels. *Energy* **36**,

5169–5179 (2011).

10. Pienkos NREL, P. T. *DOE Algal Biofuels Workshop Historical Overview of Algal Biofuel Technoeconomic Analyses*. (2008).
11. Curtis, W. R. Growing Cells in a Reservoir Formed of a Flexible Sterile Plastic Liner. (2004).
12. Tuerk, A. L. AN ASSESSMENT OF PHOTOSYNTHETIC BIOFUELS AND ELECTROFUELS TECHNOLOGIES UNDER RATE-LIMITED CONDITIONS. (Pennsylvania State University, 2011).
13. Grady, L. K. A BIOPROCESSING COMPARISON OF HIGH DENSITY BOTRYOCOCCUS BRAUNII AND CHLORELLA VULGARIS VERIFYING LIGHT LIMITED GROWTH. (The Pennsylvania State University, 2010).
14. Curtis, B. Development of Rhodobacter for the Production of Functional Membrane Proteins. (Pennsylvania State University, 2011). doi:10.13140/RG.2.1.2314.1286
15. Khatri, W., Hendrix, R., Niehaus, T., Chappell, J. & Curtis, W. R. Hydrocarbon production in high density Botryococcus braunii race B continuous culture. *Biotechnol. Bioeng.* **111**, 493–503 (2014).
16. Tuerk, A. *et al. Algae Biofuels: Slow and Steady Can Win*. (2016).
17. Rattalino Edreira, J. I. *et al.* From sunlight to seed: Assessing limits to solar radiation capture and conversion in agro-ecosystems. *Agric. For. Meteorol.* **280**, 107775 (2020).
18. Pirt, S. J., Lee, Y.-K., Richmond, A. & Pirt, M. W. The photosynthetic efficiency of Chlorella biomass growth with reference to solar energy utilisation. *J. Chem. Technol. Biotechnol.* **30**, 25–34 (1980).
19. Verlaan, P., Tramper, J., Van't Reit, K. & Luyben, K. C. H. A. M. A hydrodynamic model

for an airlift-loop bioreactor with external loop. *Chem. Eng. J.* **33**, B43–B53 (1986).

20. Hassanzadeganroudsari, M., Nakhjiri, A. T., Heydarinasab, A. & Raza, A. Modeling and Simulation of Airlift Bioreactor With External Flow Loop Using Computational Fluid Dynamic. (2018). doi:10.5281/ZENODO.2541430
21. Banerjee, A., Sharma, R., Chisti, Y. & Banerjee, U. C. Critical Reviews in Biotechnology Botryococcus braunii: A Renewable Source of Hydrocarbons and Other Chemicals. *Crit. Rev. Biotechnol.* **22**, 245–279 (2002).
22. Musiał, M., Bitenc, M. & Karcz, J. Mixing characteristics for gas-liquid system in an external-loop air-lift column. *Czas. Tech. Chem.* **R. 111**, z., (2014).
23. Bertrand, G. L. Spectrophotometry. *Missouri University of Science and Technology* 1 (2008).
24. Instrumente, T. OPT101 Monolithic Photodiode and Single-Supply Transimpedance Amplifier. (2015). Available at: https://www.ti.com/lit/ds/symlink/opt101.pdf. (Accessed: 14th April 2020)
25. Rehm, B., Consultant, D., Haghshenas, A., Paknejad, A. S. & Schubert, J. Situational Problems in MPD. in *Managed Pressure Drilling* 39–80 (Elsevier, 2008). doi:10.1016/b978-1-933762-24-1.50008-5
26. Croze, O. A., Sardina, G., Ahmed, M., Bees, M. A. & Brandt, L. Dispersion of swimming algae in laminar and turbulent channel flows: Consequences for photobioreactors. *J. R. Soc. Interface* **10**, (2013).
27. Kalpakli, A., Örlü, R. & Alfredsson, P. H. Dean vortices in turbulent flows: Rocking or rolling? *Journal of Visualization* **15**, 37–38 (2012).
28. Water Density. Available at: https://www.usgs.gov/special-topic/water-science-

school/science/water-density?qt-science_center_objects=0#qt-science_center_objects. (Accessed: 4th March 2020)

29. Kestin, J., Sengers, J. V., Kamgar-Parsi, B. & Levelt Sengers, J. M. H. Thermophysical Properties of Fluid H2O. *J. Phys. Chem. Ref. Data* **13**, 175–183 (1984).

30. Huang, Q., Jiang, F., Wang, L. & Yang, C. Design of Photobioreactors for Mass Cultivation of Photosynthetic Organisms. *Engineering* **3**, 318–329 (2017).

31. De Winter, L., Cabanelas, I. T. D., Martens, D. E., Wijffels, R. H. & Barbosa, M. J. The influence of day/night cycles on biomass yield and composition of Neochloris oleoabundans. *Biotechnol. Biofuels* **10**, (2017).

32. Myers, J. A., Curtis, B. S. & Curtis, W. R. Improving accuracy of cell and chromophore concentration measurements using optical density. *BMC Biophys.* **6**, 4 (2013).

33. Fu, W. *et al.* Maximizing biomass productivity and cell density of Chlorella vulgaris by using light-emitting diode-based photobioreactor. *J. Biotechnol.* **161**, 242–249 (2012).

34. Oukarroum, A. Change in Photosystem II Photochemistry During Algal Growth Phases of Chlorella vulgaris and Scenedesmus obliquus. *Curr. Microbiol.* **72**, 692–699 (2016).

35. Wang, J. & Curtis, W. R. Proton stoichiometric imbalance during algae photosynthetic growth on various nitrogen sources: toward metabolic pH control. *J. Appl. Phycol.* **28**, 43–52 (2016).

36. Wagner, H., Jakob, T. & Wilhelm, C. Balancing the energy flow from captured light to biomass under fluctuating light conditions. *New Phytol.* **169**, 95–108 (2006).

37. Moutafchieva, D., Popova, D. & Dimitrova, M. *EXPERIMENTAL DETERMINATION OF THE VOLUMETRIC MASS TRANSFER COEFFICIENT*. *Tchaoushev Journal of Chemical Technology and Metallurgy* **48**, (2013).

38. Hill, G. A. Measurement of overall volumetric mass transfer coefficients for carbon dioxide in a well-mixed reactor using a pH probe. *Ind. Eng. Chem. Res.* **45**, 5796–5800 (2006).

39. Sieblist, C. *et al.* Insights into large-scale cell-culture reactors: II. Gas-phase mixing and CO2 stripping. *Biotechnol. J.* **6**, 1547–1556 (2011).

40. Valdés, F. J., Hernández, M. R., Catalá, L. & Marcilla, A. Estimation of CO 2 stripping/CO 2 microalgae consumption ratios in a bubble column photobioreactor using the analysis of the pH profiles. Application to Nannochloropsis oculata microalgae culture. *Bioresour. Technol.* **119**, 1–6 (2012).

41. Ying, K., Al-Mashhadani, M. K. H., Hanotu, J. O., Gilmour, D. J. & Zimmerman, W. B. Enhanced Mass Transfer in Microbubble Driven Airlift Bioreactor for Microalgal Culture. 735–743 (2013). doi:10.4236/eng.2013.59088

42. Ndiaye, M., Gadoin, E. & Gentric, C. CO2 gas–liquid mass transfer and kLa estimation: Numerical investigation in the context of airlift photobioreactor scale-up. *Chem. Eng. Res. Des.* **133**, 90–102 (2018).

43. Yuvraj & Padmanabhan, P. Technical insight on the requirements for CO2-saturated growth of microalgae in photobioreactors. *3 Biotech* **7**, 119 (2017).

44. Haynes, W. M. *CRC Handbook of Chemistry and Physics*. (Taylor & Francis Group, 2010).

45. Tescione, L., Asplund, P. & Curtis, W. R. Reactor Design for Root Culture. in *Plant Cell and Tissue Culture for the Production of Food Ingredients* 139–156 (Springer US, 1999). doi:10.1007/978-1-4615-4753-2_13

46. Sengupta, A. & Wangikar, P. P. A method to compute instantaneous oxygen evolution

rates in cyanobacterial cultures grown in shake flasks. *Eng. Reports* **2**, (2020).

47. Sander, R. Compilation of Henry's law constants (version 4.0) for water as solvent. *Atmos. Chem. Phys* **15**, 4399–4981 (2015).

48. Liu, K. *et al.* Investigation and Modeling of Gas-Liquid Mass Transfer in a Sparged and Non-Sparged Continuous Stirred Tank Reactor with Potential Application in Syngas Fermentation. *Fermentation* **5**, 75 (2019).

49. Soleymani, T., Folan, L. M., Soter, N. A., Elbuluk, N. & Cohen, D. E. Daily indoor light exposure: A spectral analysis of ambient light sources and its relevance to occupational dermatology. *J. Am. Acad. Dermatol.* **76**, 763–765 (2017).

50. Swinehart, D. F. *The Beer-Lambert Law*. (1962).

51. Weyer, K. M., Bush, D. R., Darzins, A. & Willson, B. D. Theoretical maximum algal oil production. *Bioenergy Res.* **3**, 204–213 (2010).

52. Kula, M., Rys, M., Możdżeń, K. & Skoczowski, A. Metabolic activity, the chemical composition of biomass and photosynthetic activity of *Chlorella vulgaris* under different light spectra in photobioreactors. *Eng. Life Sci.* **14**, 57–67 (2014).

53. Metzger, P. & Largeau, C. Botryococcus braunii: A rich source for hydrocarbons and related ether lipids. *Applied Microbiology and Biotechnology* **66**, 486–496 (2005).

ACADEMIC VITA

Lucas A. Nugent

Education

The Pennsylvania State University, Schreyer Honors College *Graduation: May 2020*

B.S. Chemical Engineering

Engineering Experience

Packaging Development Intern, Mars Petcare, Franklin, TN *June – Aug 2019*

- Generated a dry food packaging design matrix based on product, process, and customer needs
- Established testing guidelines from time-accelerated models for moisture and oxidation of dry food
- Orchestrated a root-cause investigation into hot melt failures, leading to over $300K annual savings

Materials Research and Engineering Co-op, Kimberly-Clark Corporation, Neenah, WI *Jan – Aug 2018*

- Worked on the Global Absorbent Development Team for the Huggies® brand
- Collaborated with international teams to align on next steps based on research findings
- Developed a consumer-relevant test method to investigate urine-handling capabilities of diapers
- Published three reports on fundamental research for absorbent diaper core technologies
- Led a materials trial on the Absorbent Development Line at the K-C Pilot and Experimental Facility

Engineering Intern, USDA Eastern Regional Research Center, Wyndmoor, PA *May – July 2017*

- Worked on a team utilizing waste crop biomass as a petroleum substitution for fuels and co-products
- Increased the reproducibility of experimental techniques to reduce the time and cost of research
- Executed experiments using a GC-MS and elemental analysis device

Chemical Engineering Researcher, Algae Biofuels, Penn State Curtis Lab *July 2016 – Spring 2020*

- Designed, constructed and tested an algae photobioreactor to understand energy balances of biofuels
- Mentored incoming lab members in the algae department on safety and lab techniques
- Created written and videoed standard operating procedures relevant to my projects

International Product Design Program, National University of Singapore *May – June 2016*

- Prototyped a sustainable cleaning device for the NUS gutter system using an iterative process
- Worked in a multicultural team with students from various religious and ethnic backgrounds

Honors and Awards

Penn State University Montgomery County Alumni Chapter Scholarship *Fall 2017*

- Selected for scholarship based on academic performance and impact to the community

Third Place, AIChE National Undergraduate Poster Competition *Fall 2016*

- Presented a poster on algae biofuels research in the Fuels, Petrochemicals, and Energy category

President's Freshman Award *Spring 2015*

- Earned Penn State Freshman academic excellence award

First Place, General Electric Sponsored Engineering Design Competition *Fall 2015*

- Won the Most Innovative Design award for design of natural gas freight rail transportation system

Involvement and Community Service

Donations Committee Lead, Kimberly-Clark Harbor House Golf Outing *Spring - Summer 2018*

- Headed committee with goal of raising funds for domestic violence survivors through the golf outing
- Implemented a financial management system to raise over $3,000 by utilizing K-C Gift Matching
- Communicated with over 150 companies to coordinate silent auction donations worth over $2,000

The Pennsylvania State University Marching Blue Band *Fall 2015 – Spring 2017*

- Performed the trumpet for Penn State Football pregame and halftime shows

Photographer, Schreyer Honors College, State College, PA *Fall 2015 – Spring 2016*

- Photographed events for Schreyer Honors College publications and social media

Special Olympics Volunteer *Fall 2014 – Summer 2017*

- Assisted athletes in practices and swim competitions and trained new volunteers